

Junichi Takagi
Timothy A. Springer

Integrin activation and structural rearrangement

Authors' addresses

Junichi Takagi, Timothy A. Springer,
The Center for Blood Research, Departments
of Pathology and Pediatrics, Harvard Medical
School, Boston, Massachusetts, USA.

Correspondence to:

Timothy A. Springer
The Center for Blood Research
Departments of Pathology and Pediatrics
Harvard Medical School
200 Longwood Avenue
Boston, MA 02115
USA
Tel: 617 278 3225
Fax: 617 278 3232
E-mail: springeroffice@cbr.med.harvard.edu

Acknowledgments

Work in this lab was supported by NIH grants CA31798, CA31799, and HL48675. We thank our colleagues at Harvard Medical School, Motomu Shimaoka (Department of Anesthesia) and Natalia Beglova and Stephen Blacklow (Department of Pathology) for figures, and Tom Walz (Department of Cell Biology) for allowing us to cite work not yet accepted for publication.

Summary: Among adhesion receptor families, integrins are particularly important in biological processes that require rapid modulation of adhesion and de-adhesion. Activation on a timescale of < 1 s of $\beta 2$ integrins on leukocytes and $\beta 3$ integrins on platelets enables deposition of these cells at sites of inflammation or vessel wall injury. Recent crystal, nuclear magnetic resonance (NMR), and electron microscope (EM) structures of integrins and their domains lead to a unifying mechanism of activation for both integrins that contain and those that lack an inserted (I) domain. The I domain adopts two alternative conformations, termed open and closed. In striking similarity to signaling G-proteins, rearrangement of a Mg^{2+} -binding site is linked to large conformational movements in distant backbone regions. Mutations that stabilize a particular conformation show that the open conformation has high affinity for ligand, whereas the closed conformation has low affinity. Movement of the C-terminal α -helix 10 Å down the side of the domain in the open conformation is sufficient to increase affinity at the distal ligand-binding site 9000-fold. This C-terminal "bell-rope" provides a mechanism for linkage to conformational movements in other domains. Recent structures and functional studies reveal interactions between β -propeller, I, and I-like domains in the integrin headpiece, and a critical role for integrin epidermal growth factor (EGF) domains in the stalk region. The headpiece of the integrin faces down towards the membrane in the inactive conformation, and extends upward in a "switchblade"-like opening upon activation. These long-range structural rearrangements of the entire integrin molecule involving interdomain contacts appear closely linked to conformational changes within the I and I-like domains, which result in increased affinity and competence for ligand binding.

Introduction

Integrins are adhesion molecules with noncovalently associated α and β subunits that mediate cell–cell, cell–extracellular matrix, and cell–pathogen interactions. Nineteen different integrin α subunits and eight different β subunits have been reported in vertebrates (1,2), forming at least 25 $\alpha\beta$ heterodimers and perhaps making the integrins the most structurally and functionally diverse family of cell adhesion molecules. These integrins differ with respect to which cell sur-

Immunological Reviews 2002

Vol 186: 141–163

Printed in Denmark. All rights reserved

Copyright © Blackwell Munksgaard 2002

Immunological Reviews
0105-2896

face, extracellular matrix, or inflammatory ligands they bind, the mechanisms by which their binding activity for ligands is activated, the types of cytoskeletal components to which they bind, and the types of signaling pathways that they activate within cells.

The most unusual feature of integrins compared to other adhesion molecules is that the ability of their extracellular domains to bind ligands can be activated on a timescale of < 1 s by signals within the cell (inside-out signaling). This is particularly evident with integrins on platelets and leukocytes in the bloodstream. Activation of integrins on these cells enables platelets to bind to injured vessel walls and fibrin clots, and enables leukocytes to bind to vessel walls and subsequently to migrate across the endothelium to participate in immune and inflammatory processes. Multiple mechanisms including conformational change in integrins (affinity regulation), and clustering and association with the cytoskeleton (avidity regulation), have been proposed to explain these events (3–10). There is abundant evidence obtained using antibodies for conformational change in many of the different extracellular integrin domains. However, it has been questioned whether conformational change is a result of ligand binding or a cause of ligand binding (affinity regulation). Multiple structures have been determined for the inserted (I) domain that is a key ligand-binding domain in many integrins. I domains became embroiled in similar controversies as to whether conformational differences seen in crystal structures were physiologically relevant, and whether conformational change could regulate ligand binding or was merely a consequence of ligand binding. Now, through mutational and further structural studies, it is clear that conformational change in integrin I domains is of key physiologic importance for regulating the affinity for ligand. Recently, the structure of the extracellular fragment of integrin $\alpha V\beta 3$, which lacks an I domain, was reported at 3.1-Å resolution (11). It was a big surprise for integrin researchers that this structure assumed a bent conformation, in which the ligand-binding headpiece is folded back onto the tailpiece of the molecule. This picture is completely different from what was expected from the electron micrograph images known for years, which show a conformation in which the headpiece is extended far away from the membrane on two long stalks (12–15). A small molecule antagonist can be soaked into the crystals and bind to the bent conformation (16). Nonetheless, the suggestion by the authors of the crystal structure paper that the bent structure represents the active conformer (11) was puzzling, since the ligand-binding site would face back toward the membrane surface, in an orientation that would be unfavor-

able for binding to ligands on other cells or in the extracellular matrix. We have recently shown, utilizing image processing of negatively stained electron micrographs and designed conformation-stabilizing mutations, that the bent form represents the inactive receptor, and that activation results in straightening of the heterodimer (17). This review focuses on exciting recent advances in the elucidation of the conformational regulation of ligand binding by integrins in general and I domains in particular, and emphasizes “structural rearrangement” as a unifying theme for activation of both integrins that contain and those that lack I domains.

An overview of integrin domain structure

Integrins contain two noncovalently associated, type I transmembrane glycoprotein α and β subunits with extracellular domains of >940 and >640 residues, respectively (Fig. 1). The intracellular domains are short, except for the cytoplasmic domain of integrin $\beta 4$, which is specialized to connect to the keratin cytoskeleton and contains fibronectin type III domains (18). A globular headpiece binds ligand, and two long stalk regions containing C-terminal segments from the α and β subunits connect the ligand-binding headpiece to the transmembrane and C-terminal cytoplasmic domains. Twelve extracellular domains are present in integrins that lack I domains; the structure of the extracellular fragment of integrin $\alpha V\beta 3$ (11) defines eight of these and a portion of a ninth. A complementary NMR structure of a $\beta 2$ integrin fragment (19) reveals the structure of some of the missing domains.

The α subunit

The N-terminal region of the integrin α subunit contains seven segments of about 60 amino acids each that have weak homology to one another, and they have been predicted to fold into a seven-bladed β -propeller domain (20) (Fig. 1). The trimeric G-protein β subunit contains a β -propeller domain with the same topology. The β -propeller model has received strong support from mapping of epitopes that are far apart in sequence but close in the predicted structure (21), and from the finding that Ca^{2+} -binding motifs in propeller β -sheets 4–7 are more similar to motifs found in turns between β -strands than to EF-hand motifs in turns between α -helices (22). Mutagenesis studies show that ligand-binding residues cluster to one portion of the “top” and “side” of the β -propeller (23). The $\alpha V\beta 3$ crystal structure is in agreement with these conclusions (11).

Half of integrin α subunits contain a domain of about 200 amino acids known as an inserted (I) domain or a von Wille-

brand factor A domain. I domains are the major ligand-binding sites in integrins that contain I domains (24,25). The I domain is inserted between β -sheets 2 and 3 of the β -propeller domain (20) (Fig. 1). The three-dimensional structure of the I domain (26) shows that it adopts the dinucleotide-binding or Rossmann fold. A divalent cation coordination site, designated the metal ion-dependent adhesion site (MIDAS) in the I domain, binds negatively charged residues in ligands.

The region C-terminal to the β -propeller domain comprises a large portion of the α subunit extracellular domain of about 500 residues. Much of this C-terminal region appears to correspond to the stalk region visualized in electron micrographs, and it is predicted to consist of domains with a two-layer β -sandwich structure (27). The crystal structure reveals the presence of three β -sandwich domains in this region, designated the thigh, calf-1, and calf-2 domains (11) (Figs 2A,B).

The β -subunit

The N-terminal cysteine-rich region of residues 1–50 shares sequence homology with membrane proteins including plexins, semaphorins, and the c-met receptor; it has therefore

been termed the PSI domain for plexins, semaphorins and integrins (28). This region in integrin β -subunits has seven cysteines, six of which are shared with other PSI domains, and the region is predicted to have two α -helices. The first of the seven cysteines forms a long-range disulfide to the C-terminal cysteine-rich region in the β -subunit (Fig. 1) (29). These cysteine-rich regions cooperate to restrain the integrin in the inactive conformation (30).

Integrin β subunits contain an evolutionarily conserved domain of about 240 residues, spanning approximately residues 100–340. This domain contains a putative metal-binding DXSXS sequence motif similar to that of the MIDAS in the I domain, a similar secondary structure (26), and weak but detectable sequence homology to the I domain (31); therefore, it has been termed the I-like domain. This region is a hotspot for point mutations that result in a lack of association of the integrin $\beta 2$ subunit with α subunits, or loss of function, and cause leukocyte adhesion deficiency. The I-like domain appears to directly bind ligand in integrins that lack I domains, and to indirectly regulate ligand binding by integrins that contain I domains. There is a large interface be-

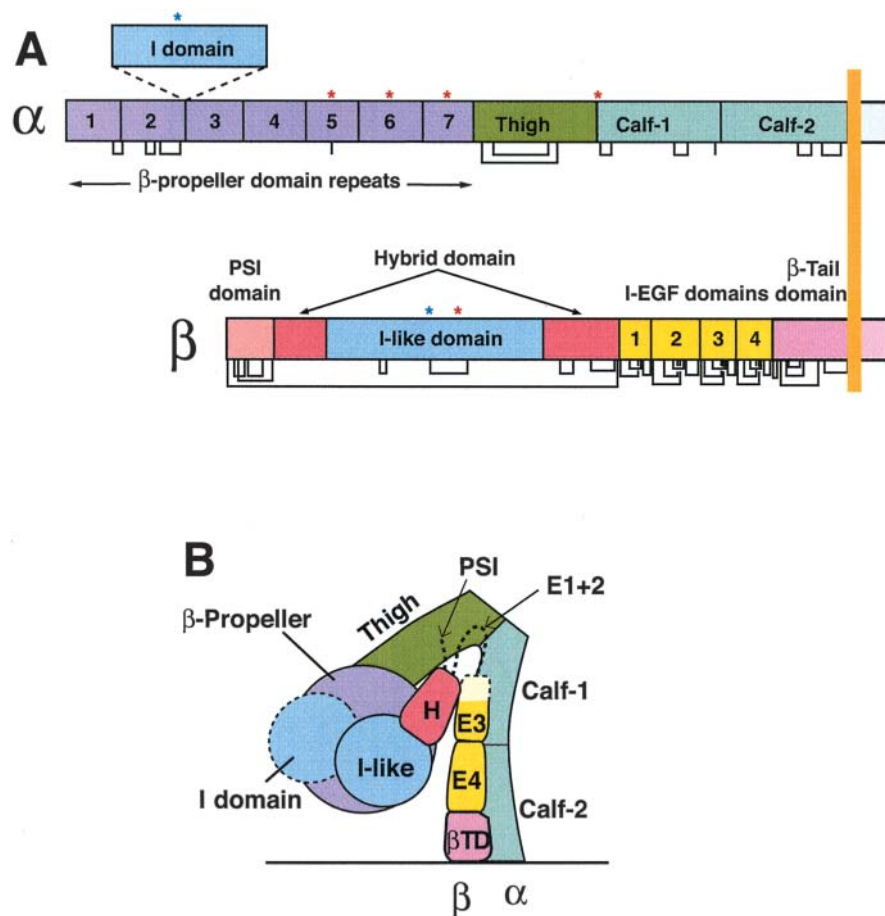


Fig. 1. Integrin architecture.

A) Organization of domains within the primary structure of integrin. Depending on the α subunit, it may contain an I-domain insertion as denoted by the dotted line. Asterisks show Mg^{2+} (blue) and Ca^{2+} (red) binding sites. Lines below the stick diagrams show disulfide bonds. **B)** Arrangement of domains within the three-dimensional crystal structure of $\alpha V\beta 3$ (11), with an I domain added. Each domain is color coded as in (A).

tween the β -propeller domain and the I-like domain (11), as originally deduced by their mutual dependence for folding (32,33) and from antibody epitopes (34,35).

The hybrid domain is a β -sandwich domain that is folded from amino acid sequence segments on either side of the I-like domain (Fig. 1). Therefore, there are two covalent connections between the I-like and hybrid domains. Interestingly, there are also two covalent connections between the I domain and the β -propeller domain in the α -subunit. Movement of one of these connections relative to the other may be an important mechanism for relating conformational change within domains to a change in the orientation between neighboring domains in both the α and β subunits, and hence in propagating global conformational changes within integrins.

From approximately residue 435 to residue 600 are four cysteine-rich repeats that are EGF-like (11,19,36–38). These

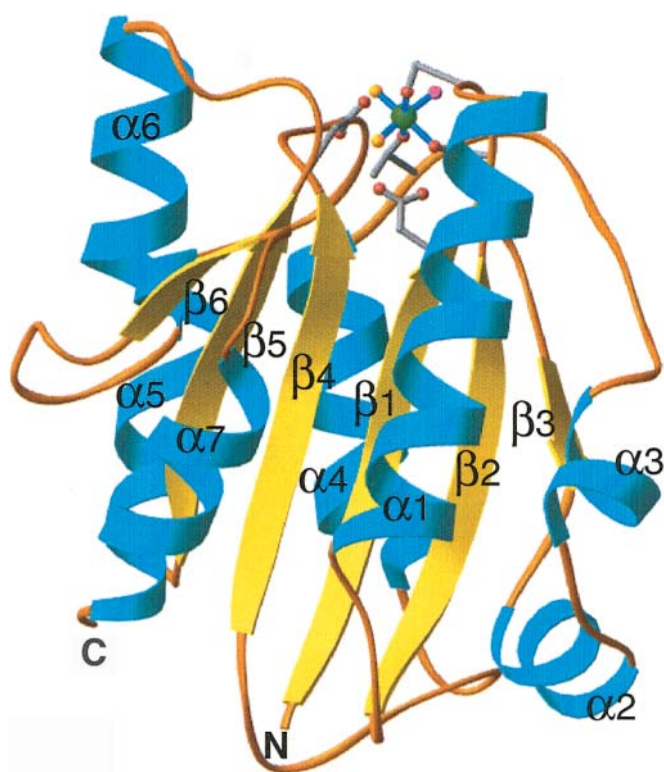


Fig. 2. Ribbon diagram of the α M I domain in the open conformation. The β -strands (yellow), α -helices (cyan), and N- and C-termini are labeled. The Mg ion is shown as a green sphere. Sidechains of residues that form primary or secondary coordinations to the metal ion (D140, S142, S144, T209 and D242) are shown with gray bonds and carbon atoms and red oxygen atoms. Coordinating water molecule oxygens are gold, and the oxygen of the ligand-mimetic Glu from another I domain is magenta. All ribbon diagrams in this review were prepared with ribbons (110).

have been designated integrin-EGF (I-EGF) domains because they have unique structural properties that make the inter-module connection rigid and suited for transmission of structural motion in signaling (19,37). Many activating antibodies, or antibodies that bind only when integrins are activated, bind to the C-terminal region of the β 1, β 2 and β 3 subunits (2). Mapping in more detail shows that these monoclonal antibodies (mAbs) map within the EGF-like modules (39). The β -tail domain is also cysteine-rich, and contains an α -helix disulfide-linked to a β -sheet.

Conformational activation of integrin I domains

I domain structure

Crystal and nuclear magnetic resonance (NMR) structures have been determined for I domains from the integrin α M (26,40,41), α L (42–45), α 2 (46,47), and α 1 (48,49) subunits. The I domain adopts the dinucleotide-binding or Rossmann fold, with α helices surrounding a central β -sheet (Fig. 2). There are six major α -helices, and several short α -helices that differ between I domains. The β -sheet contains five parallel and one antiparallel β -strand. β -strands and α -helices tend to alternate in the secondary structure, with the α -helices wrapping around the domain in counterclockwise order when viewed from the top (Fig. 2). A divalent cation sits on the top of the domain, ligated by five sidechains located in three different loops. The first of these loops, β 1- α 1, contains three coordinating residues in a sequence that is a signature of I domains, DXSXS. Divalent cations have long been known to be universally required for ligand binding by integrins, and in I domains the metal-coordinating residues, and the residues surrounding the metal-binding site, are important for ligand binding. Therefore, this site has been designated the metal ion-dependent adhesion site (MIDAS) (26). Many of the proteins with dinucleotide or Rossmann folds are enzymes that have an active site and a Mg^{2+} -binding site at the top face, and the Mg^{2+} often coordinates the phosphate group of NAD, ATP, or GTP, which are substrates or cofactors for these enzymes. Of these proteins, the most closely related to integrin I domains are the small G-proteins such as ras. The I domain and small G-protein folds differ only in one α -helix and in a reversal of the order of the β 2 and β 3 strands in the β -sheet. The structural relationship of the integrin I and I-like domains to G-protein α subunits, and of the integrin β -propeller domain to G-protein β subunits, is quite interesting and may reflect functional similarities in conformational regulation of ligand binding (11,20,40).

Two different conformations for integrin I domains
Early on, the integrin α M I domain was found to crystallize in two different conformations (40). There was considerable controversy about whether the different conformations were physiologically relevant or were an artifact of the lattice contacts in crystals (41,50). The two conformers were at first termed the Mn²⁺ and Mg²⁺ forms, because they were crystallized in the presence of these metals and bound them at the MIDAS. Later, they were termed the closed and open conformers, respectively. The latter terminology is much less confusing. Further studies have shown that the closed conformation can be seen with Mg²⁺, Mn²⁺, Cd²⁺, or no metal in the MIDAS (41,43), and the open conformation can be seen with Mg²⁺ (26), Co²⁺, Zn²⁺, and probably Mn²⁺, Cd²⁺, and Ni²⁺ in the MIDAS (47). What clearly distinguishes the closed and open I domain conformations

is that, in the two open structures determined, an acidic residue donated either by a ligand (47) or by a ligand-mimetic lattice contact (26) coordinates to the metal in the MIDAS, whereas there is no ligand-like contact in the large number of closed structures that have been determined. Instead, a water molecule is present at the equivalent coordination position (Fig. 3A). The closed and open conformations differ not only in the coordination of residues in the I domain with the MIDAS but also in the structure of surrounding loops and in the position of the C-terminal α -helix (Fig. 4A).

At the MIDAS, five residues in the I domain and several water molecules contribute oxygen atoms to the primary and secondary coordination spheres surrounding the metal (Fig. 3A). In the open conformation of the MIDAS, two serines and one threonine are in the primary coordination sphere,

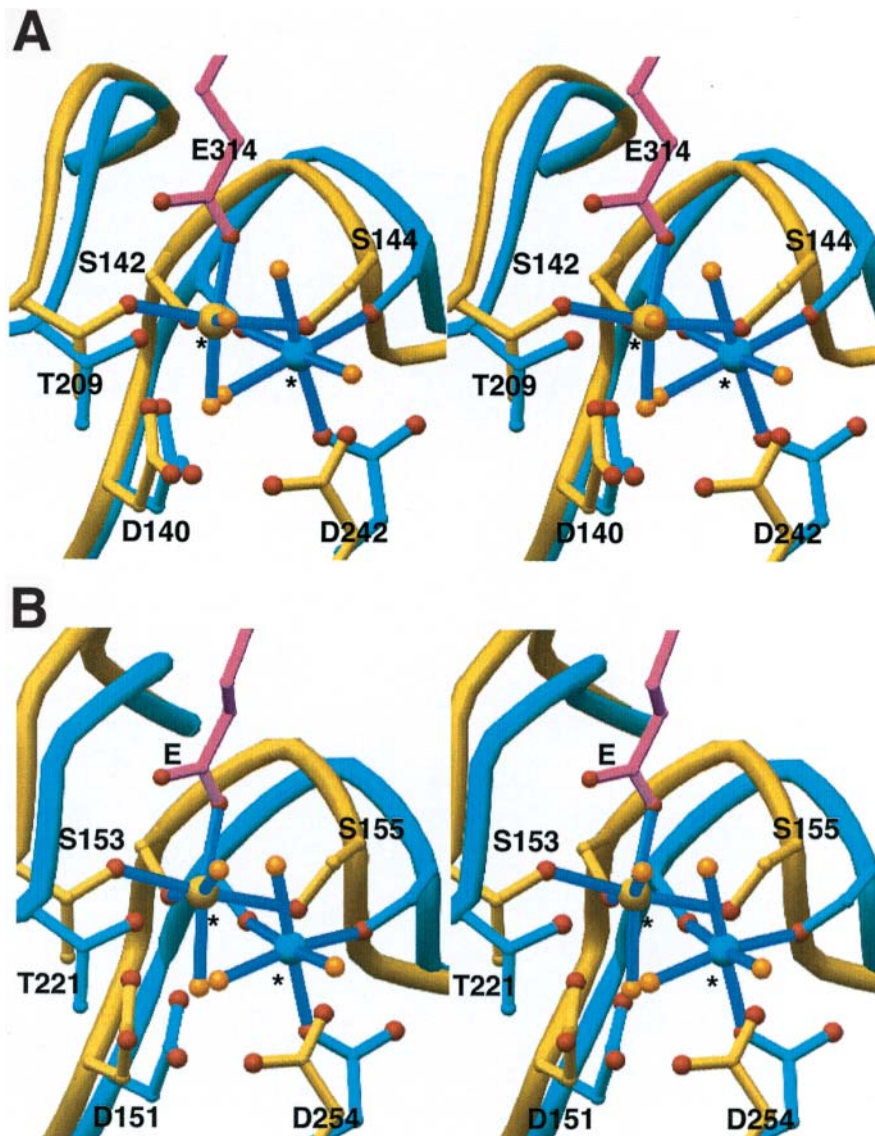


Fig. 3. Stereo view of alternative conformations of the MIDAS. A) α M. B) α 2. The backbone, coordinating sidechain bonds, and metals (labeled with asterisks) are shown in yellow (open conformation) and cyan (closed conformation). The coordinating glutamate residue bonds from the ligand-mimetic neighboring α M I domain (E314) in α M and collagen peptide ligand (E) in α 2 are in magenta. Primary coordination bonds to the metals are in blue. Oxygen atoms of the coordinating sidechains and water molecules are red and gold, respectively. I domains were superimposed on one another in turn, so all were in the same orientation as the closed 1JLM α M structure (26). The 1IDO open α M structure (40) was superimposed on 1JLM using residues 132–141, 166–206, 211–241, 246–270, and 287–294. The 1AOX closed α 2 structure (46) was superimposed on 1JLM using residues 145–153, 180–189, 192–199, 222–240, 246–256, and 268–282. The 1DZI open α 2 structure (47) was then superimposed on 1AOX using residues 143–152, 173–216, 223–253, and 259–282.

whereas two aspartic acid residues are in the secondary coordination sphere and fix the positions of coordinating water molecules (Fig. 3A). Notably, the glutamic acid contributed by the ligand-mimetic residue donates the only negatively charged oxygen to the primary coordination sphere in the open conformation. The lack of any charged group in the primary coordination sphere donated by the I domain is hypothesized to enhance the strength of the metal–ligand bond. By far the most important binding residue in intercellular adhesion molecule (ICAM)-1, the ligand for Mac-1, is a glutamic acid residue that maps to near the center of the binding site; therefore, this residue has been hypothesized to directly coordinate to a Mg^{2+} in the I domain MIDAS (51).

In the closed conformation of the I domain, the threonine moves from the primary to the secondary coordination sphere, and one of the aspartic acid residues moves from the secondary to the primary coordination sphere (Fig. 3A). This

movement is consistent with the idea that an energetically favorable MIDAS requires at least one primary coordination to a negatively charged oxygen, and when this is not provided by a ligand, there is a structural rearrangement within the I domain to provide this from within the MIDAS. The backbone and sidechain rearrangements in the I domain are accompanied by a 2.3-Å “sideways” movement of the metal ion away from the threonine and toward the aspartic acid on the opposite side of the coordination shell (Fig. 3A). A water molecule takes the place of the ligand-mimetic glutamic acid to complete the coordination sphere.

The structural rearrangement of the MIDAS is coupled to backbone movements of the loops that bear the coordinating residues. Linked structural shifts occur in neighboring loops on the top of the I domain, and there are also linked movements in α -helices on the “side” of the domain, and in the hydrophobic core (Fig. 4A). In the largest movement in the

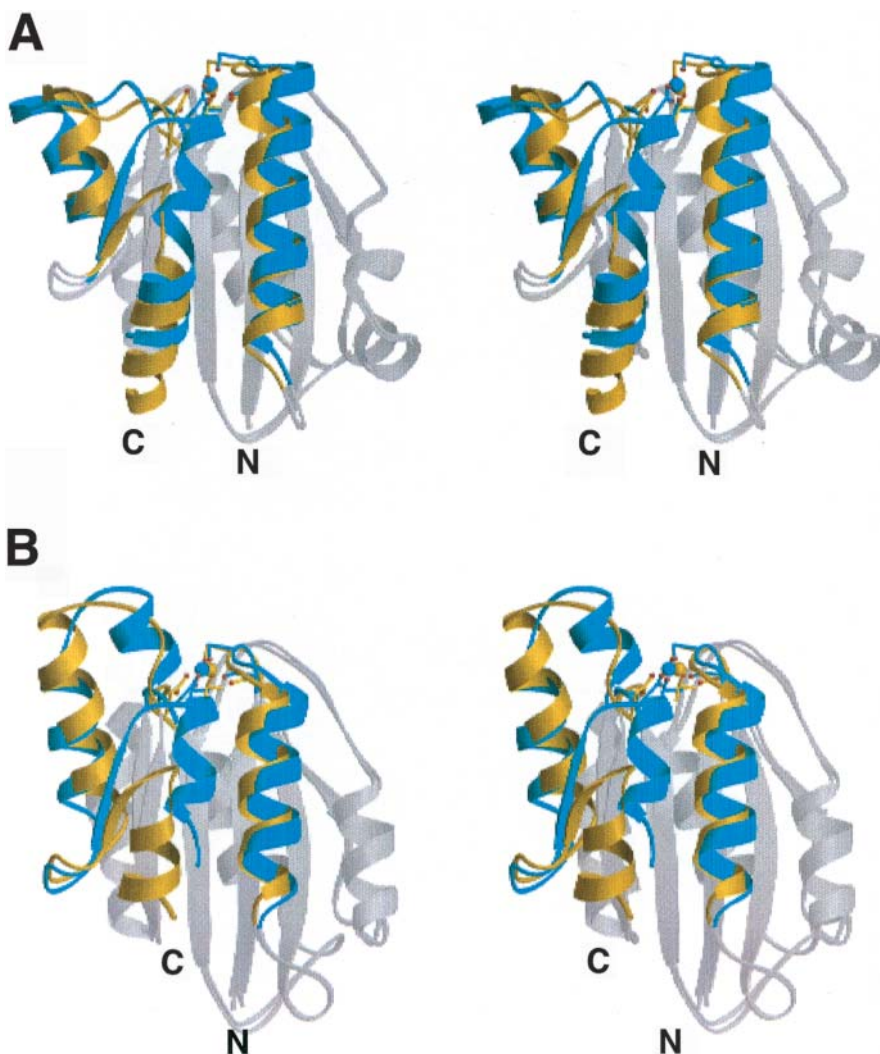


Fig. 4. Stereo view of the alternative conformations of I domains. A) αM I domain. **B)** $\alpha 2$ I domain. The regions of significant difference between the superimposed conformers are shown in yellow (open or active) and cyan (closed or inactive). Similar backbone regions are in gray. Metal atoms and coordinating sidechain bonds and carbon atoms are in yellow (open or active) and blue (closed or inactive); oxygen atoms are red. The coordinating residues are S142, S144, T209, and D242 in αM , and S153, S155, T221 and D254 in $\alpha 2$. The I domains were superimposed as in Fig. 3. The I domains in **(A)** and **(B)** are in identical orientations.

transition from the closed to the open structure, the C-terminal helix, $\alpha 7$, moves 10 Å down the side of the domain. This requires a repacking of the hydrophobic face of $\alpha 7$ against the side of the domain. At the N-terminus of $\alpha 7$, Phe-302, which inserts into a hydrophobic cavity in the top of the closed domain, becomes completely exposed as a consequence of the dramatic reshaping of the $\beta 6$ - $\alpha 7$ loop (Fig. 5). The $\alpha 7$ helix is distant from the ligand-binding site; however, its remarkable movement provides a mechanism to link conformational movements in I domains to movements elsewhere in integrins.

The structure of the $\alpha 2$ I domain has been determined in the absence of ligand (46) and in the presence of a collagen peptide ligand (47). The triple helical collagen peptide contains a critical Gly-Phe-hydroxyPro-Gly-Glu-Arg sequence, and the Glu of this sequence ligates the MIDAS. The differences between the ligand-bound and nonliganded $\alpha 2$ I domains are remarkably similar to the differences between the αM I domains with and without a ligand-mimetic lattice contact (Fig. 4B); when the differences in C α carbon backbone positions are plotted, they are remarkably similar (47). Furthermore, exactly the same changes are seen in the residues that make primary coordinations to the metal at the MIDAS (Fig. 3B). Thus, the liganded and nonliganded conformations of the $\alpha 2$ I domain adopt the open and closed conformations, just as seen for αM (Fig. 4B). The I domains of $\alpha 2$ and αM are only 27% identical in sequence and are among the most distantly related of integrin I domains; thus, it is to be expected that the open and closed conformations will be a general feature of integrin I domains.

The $\beta 6$ - $\alpha 7$ loop adopts conformations that are canonical for the open and closed structures. In the open conformations, the backbone conformations of the $\beta 6$ - $\alpha 7$ loops are almost identical in αM and $\alpha 2$ (Fig. 5). The conformation is quite different in the closed conformation, yet it is almost identical for αM and $\alpha 2$, as well as for αL and $\alpha 1$ (Fig. 5).

Is shape-shifting in integrin I domains physiologically relevant for regulation of their affinity for ligand?

The above studies demonstrated that conformational changes occur when ligands are bound to I domains. However, they did not establish whether these changes result from induced fit upon ligand binding, or whether they are physiologically relevant for regulating the affinity for ligand of I domains and the integrins in which they are present. These have been hotly debated issues in the integrin field. For some years, it has been proposed that, after cellular activation, signals are transmitted to the extracellular domains of integrins that alter the

conformation of their ligand-binding site, and hence affinity for ligand (4,52). More recently, evidence has also accumulated that lateral redistribution and clustering of integrins, or so-called avidity regulation, may alter cellular adhesion independently of a change in affinity for ligand (8). Indeed, it has been suggested that conformational change in integrins is overemphasized and that it is a consequence rather than a cause of ligand binding (9). The binding of many antibodies to integrins is stabilized or induced by ligands, leading to the term “ligand-induced binding sites” or “LIBS” for these epitopes. Although many of the same antibodies can “activate” ligand binding, this activation can be argued to be a consequence of stabilizing the ligand-bound conformation and hence the integrin–ligand complex. The keys to resolving

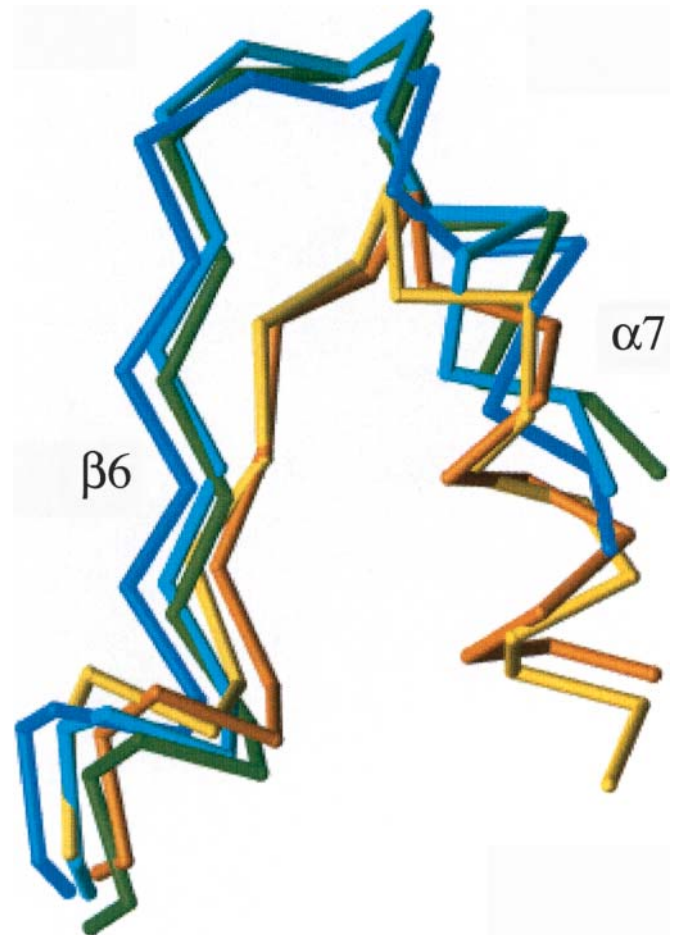


Fig. 5. The loop between the most C-terminal β -strand ($\beta 6$) and α -helix ($\alpha 7$) in I domains has a canonical conformation in open structures and a different canonical structure in closed structures. Loops are shown for open (αM , yellow; $\alpha 2$, gold) and closed (αM , blue; $\alpha 2$, green; αL , dark blue) conformations. For clarity, only residues 290–310 of αM , 306–326 of $\alpha 2$, and 280–300 of αL , which are of equal length in the closed and open structures and in all three I domains, are shown. I domains were superimposed as described in Fig. 3.

these issues were (i) whether the conformational changes seen in crystal structures were physiologically relevant, i.e. altered affinity for ligand as predicted, (ii) whether the change in affinity was substantial, and (iii) whether conformational alterations in I domains occurred on the cell surface in physiological circumstances.

Many mAbs to integrins have been reported that either bind only when the integrin is activated, or induce activation themselves (9). However, very few activation-dependent mAbs block ligand binding, and thus appear to recognize the ligand-binding site. The only such mAb to I domains reported is CBRM1/5, which recognizes the I domain of α M (53). This mAb does not bind to resting peripheral blood neutrophils, but after these cells are activated through G-protein-coupled chemoattractant receptors, or with a drug that activates protein kinase C, 10 or 30%, respectively, of the α M β 2 molecules on the surface of individual cells binds CBRM1/5 mAb. Although it recognizes only a subset of the α M β 2 molecules on the cell surface, CBRM1/5 mAb completely blocks ligand binding by cells, showing that it recognizes the active subset of molecules.

Evidence to support the physiological relevance of confor-

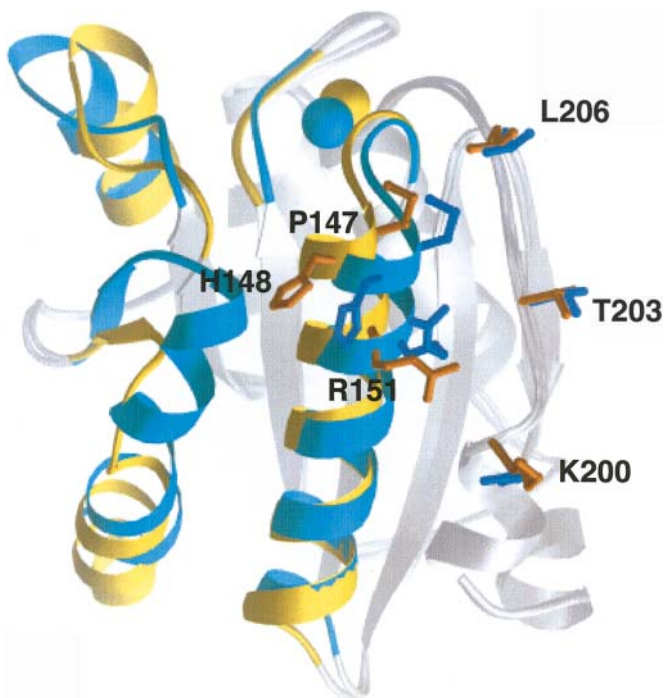


Fig. 6. Alteration of the CBRM1/5 epitope in open and closed α M I domains. The metals and regions where conformational changes are significant are shown in yellow (open) and blue (closed). Other backbone regions are gray. Sidechains of the CBRM1/5 epitope are in gold (open) and dark blue (closed). The open and closed α M I domain structures were superimposed as described in Fig. 3.

mational change seen in the open and closed forms of α M I domain crystal structures was provided by CBRM1/5 mAb (54). This mouse antihuman mAb is specific for six residues that differ between the human and mouse amino acid sequences. The residues in the epitope are present in two different amino acid segments that are structurally adjacent and near the MIDAS (54) (Fig. 6). The first three residues, P147, H148 and R151, are located at the top of the α 1 helix and are preceded immediately by three of the residues that coordinate the Mg^{2+} and form the DXSXS motif of the MIDAS: D140, S142, and S144. The last three residues, K200, T203 and L206, are in the loop that contains T209, which is directly coordinated to the metal in the open conformation and indirectly coordinated in the closed conformation. Both groups of residues are widely exposed regardless of activation as judged by reactivity with other antibodies. These results suggest that the selectivity of CBRM1/5 for the active state is not a consequence of “unmasking” of the epitope by other integrin domains but of “shape-shifting” in the I domain itself. This conclusion is supported by studies with isolated I domains (see below, and M. Shimaoka and T. A. Springer, unpublished data). Comparison between the superimposed open and closed structures shows that P147, H148 and R151 differ markedly in position and in sidechain orientation, and hence in relationship to the three other residues in the epitope (Fig. 6). α atom movements that average 2.4 Å are tightly linked to the 2.0-Å movement of S144 of the MIDAS. Additionally, H148 and R151 are adjacent to the loop preceding the C-terminal α -helix in the closed conformation, and both are more exposed in the open conformation, as a result of the movement of this loop that accompanies the large downward shift of the C-terminal α -helix. Thus, CBRM1/5 recognizes shape-shifting in the α M I domain near the MIDAS and the C-terminal α -helix. Documentation of shape-shifting in these regions of the I domain upon activation of integrins on the cell surface provides strong evidence that conformational change seen in the open and closed I domain structures is physiologically relevant, and occurs within the context of intact integrin $\alpha\beta$ heterodimers. Since CBRM1/5 mAb blocks ligand binding, it clearly does not recognize a ligand-induced binding site (LIBS). Therefore, the induction of the CBRM1/5 epitope on cell surface α M β 2 is a consequence of changes within α M β 2 itself, and not of ligand binding.

Mutations that stabilize the open or closed conformers of I domains

To measure how transition between the open and closed conformations of the I domain regulates affinity for ligand, muta-

tions have been introduced to stabilize a particular conformation, and tested for effect on ligand binding. Both the open and closed conformations of the α M I domain were stabilized with different mutations to investigate the physiological significance of these conformations (55). The computational algorithm orbit, developed by Mayo and colleagues (56), rationally designs amino acid sequences that stabilize a particular backbone structure. Using orbit, sequences were selected that minimized the energy of either the open or closed conformation of the α M I domain. Back calculations showed that mutations that stabilized the open conformation also destabilized the closed conformation, and vice versa. To avoid mutations that could directly alter the ligand-binding face or alter contacts with other domains in intact integrins, only hydrophobic core residues were allowed to mutate. Three different designed open I domains, which contained 8–13 mutations each, showed increased binding to ligand when expressed on the cell surface in α M β 2 heterodimers, whereas designed closed or wild-type I domains did not (55). Similar results were obtained when I domains alone, in the absence of any other integrin domains, were expressed on the cell surface with an artificial C-terminal transmembrane domain. The CBRM1/5 mAb reacted with α M β 2 containing the designed open but not designed closed or wild-type I domains. Furthermore, α M β 2 heterodimers containing wild-type, but not designed closed I domains, bound ligand in response to activating mAb, showing that the closed I domain was resistant to activation. These results demonstrated that the open and closed conformations correspond to ligand-binding and inactive conformations, respectively.

The closed conformation appears to be the low-energy conformation of the I domain and to be the default conformation adopted by the I domain in resting integrin heterodimers on the cell surface. In α M β 2 heterodimers, and in isolation on the cell surface, the wild-type I domain behaved like the designed closed I domain in lack of expression of the CBRM1/5 epitope and lack of ligand binding. This suggests that the closed conformation is adopted in the inactive state by integrins on the cell surface. Calculation of the energies of α M I domains crystallized in the open and closed conformations also shows that the closed conformation is of lower energy (55).

Mutation in the α M I domain of the single residue Ile-316, located in the second half of the C-terminal α -helix, is sufficient to favor the open conformation (57). The sidechain of Ile-316 packs in a hydrophobic pocket between the C-terminal α -helix and the opposing β -sheet in the closed conformation, but, because of the downward movement of this

helix in the open conformation, this residue cannot pack against the side of the domain in the open conformation and is not visualized in the crystal structure of the open conformer (40). To test the hypothesis that packing of Ile-316 wedged into this hydrophobic socket might constrain the α M I domain in the closed conformation, recombinant soluble α M I domains were truncated just before Ile-316 (r11b^{A123-315}) or Ile-316 was mutated to Gly (r11b^{Alle-316-Gly}) (57). These mutants showed increased affinity for the ligands iC3b, fibrinogen and ICAM-1, compared to the wild-type I domain (r11b^{A123-321}), as revealed by surface plasmon resonance (57). Thus, the absence of the Ile-316 sidechain clearly favors the open, ligand-binding conformation in solution. The r11b^{Alle-316-Gly} mutant crystallized in the open conformation when a ligand-mimetic crystal contact was present. However, since the wild-type r11bA123-315 also crystallized in the open conformation when a ligand-mimetic crystal contact was present (57), as also observed in the first α M I domain crystal structure (26), the crystal studies do not reveal which conformation is present in solution, and they do not reveal whether the Ile-316 mutation by itself is sufficient for conversion to the open conformation in the absence of a ligand-mimetic contact.

Locking the α L I domain in the open conformation (58–60) has relied on models, since all α L structures thus far show the closed conformation (42–45). The open conformation of the α L I domain was modeled by using the structure of the open α M I domain as a template in regions where the closed and open conformations differed. Positions were sought where pairs of residues could be mutated to cysteine that could form a disulfide bond, and the disulfide could form only in one conformation. The positions that were found bracket the loop between the C-terminal α -helix and preceding β -strand (Fig. 7). To lock this loop in its two alternate conformations, pairs of cysteines were introduced either at residues 287 and 294 for the open conformation, or at residues 289 and 294 for the closed conformation. In surface plasmon resonance measurements of binding to ICAM-1, the soluble locked open α L I domain molecule showed a 9000-fold increase in affinity compared to wild type, which was reversed by disulfide reduction. Locking the I domain open increases its on-rate, which is consistent with conformational change being rate-limiting for binding of the wild-type I domain (Table 1). The affinity of the locked closed conformer was similar to that of wild type (58). Furthermore, the affinity and kinetics of the soluble locked open α L I domain for ICAM-1 were comparable to those measured independently (61) for intact, activated α L β 2 (Table 1). Thus, the α L I do-

main, when locked in the open conformation, is sufficient for full affinity binding.

The locked open and closed I domains were also tested for adhesiveness in the context of intact $\alpha\text{L}\beta\text{2}$ on the cell surface (59). $\alpha\text{L}\beta\text{2}$ containing the locked open I domain was constitutively and maximally active for adhesion to ICAM-1, while

$\alpha\text{L}\beta\text{2}$ heterodimers containing wild-type or locked closed I domains failed to support adhesion. $\alpha\text{L}\beta\text{2}$ containing the wild-type I domain was activatable for adhesion by activating mAb or Mn^{2+} , while $\alpha\text{L}\beta\text{2}$ containing the locked closed I domain was resistant to such activators. The results with soluble I domains and cell surface heterodimers clearly demonstrated

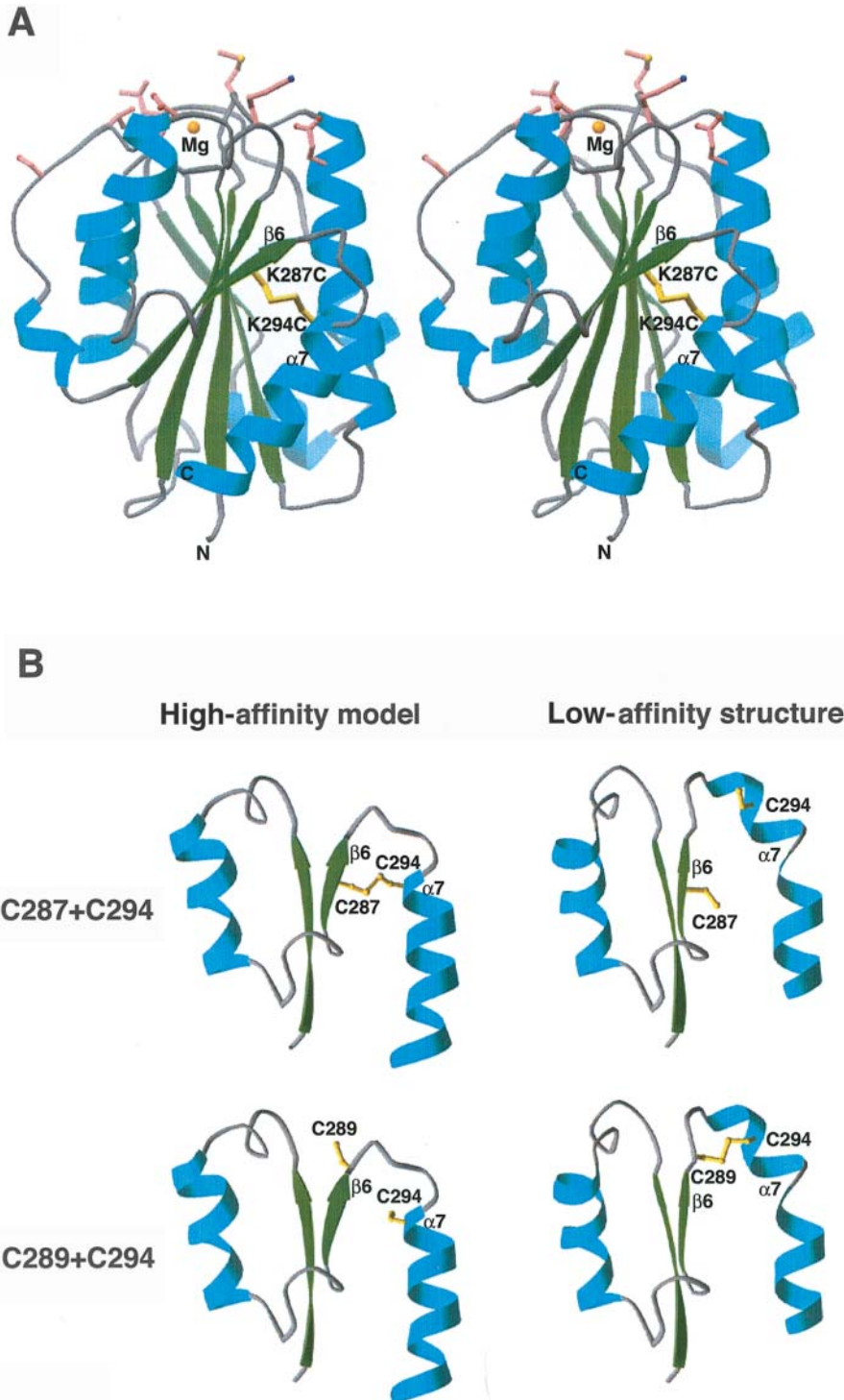


Fig. 7. Locking in αL I domain conformations with engineered disulfide bridges. **A)** Stereodialog of the high-affinity model of the αL I domain, with mutations to introduce a disulfide bond. The sidechains and disulfide bond of C287 and C294 are shown in yellow. The Mg^{2+} ion of the MIDAS is shown as a gold sphere. Sidechains of residues important in binding to ICAM-1 and ICAM-2 are shown with rose-pink sidechains and yellow sulfur, red oxygen, and blue nitrogen atoms. These residues, defined as important in species-specific binding to ICAM-1 (79) or by at least a 2-fold effect on binding to ICAM-1 or ICAM-2 upon mutation to alanine (111), are M140, E146, T175, L205, E241, T243, S245, and K263. Note that these residues surround the Mg^{2+} ion, and are distant from the disulfide.

B) Predicted disulfide bonds that are selective for open or closed conformers of the αL I domain. The K287C/K294C mutation (upper panels) and L289C/K294C mutation (lower panels) were modeled in both open (high-affinity model, left panels) and closed (low-affinity structure, right panels) I domain conformers. For clarity, only residues 254–305 of the models are shown. The four models were superimposed using residues not involved in conformational shifts and are shown in exactly the same orientation. The downward movement of the α7 helix in the left panels compared to the right panels is readily apparent. The remodeling of the loop connecting β6 and α7 is accompanied by a reversal in the orientation of the sidechain of residue 289. Figure from ref (58).

that reshaping of the $\beta 6$ - $\alpha 7$ loop is fully sufficient for regulation of the affinity of the ligand-binding site at the MIDAS, because only the conformation of the $\beta 6$ - $\alpha 7$ loop is directly restrained by the disulfide bond. Therefore, inside-out signals relayed from the cytoplasm could be propagated to the ligand-binding site, by pulling down the C-terminal $\alpha 7$ helix, and thereby reconfiguring the $\beta 6$ - $\alpha 7$ loop.

As discussed above, controversy has surrounded the contribution to regulation of adhesiveness of lateral movements on the cell surface (clustering, avidity regulation) and conformational change in the ligand-binding site (affinity regulation). In part to address this issue, I domains were expressed on the cell surface in isolation from other integrin domains using an artificial transmembrane domain (59). In contrast to native $\alpha L\beta 2$, the cell surface I domains contained only a single transmembrane domain, derived from the platelet-derived growth factor receptor and truncated five residues into the cytoplasmic domain. Isolated wild-type or locked closed I domains did not support adhesion, while the isolated locked open I domain was as strongly adhesive for ICAM-1 as fully activated intact $\alpha L\beta 2$ heterodimer at an equivalent cell surface density. These findings demonstrate that affinity regulation is fully sufficient to regulate cell adhesiveness, and that interactions between integrins or other components mediated by integrin cytoplasmic, transmembrane, or any extracellular domains other than the I domain are not required. However, these findings do not rule out a role for avidity regulation or a link between conformational change in integrins and clustering.

Mutations around the interface between the C-terminal α -helix and the opposing β -sheet affect ligand-binding activity, underscoring the significance of conformational changes occurring around the C-terminal α -helix. Systematic mutagenesis of this region has revealed mutations that both increase and decrease ligand binding by $\alpha L\beta 2$, apparently by affecting the relative stability of the open and closed conformations, or by affecting interactions with nearby domains that regulate I domain conformation (62). One of these residues, Ile-306, corresponds to Ile-316 of αM which, as described above, stabilizes the closed conformation by fitting in a hydrophobic socket (57). Consistent with the observations with the αM I

domain, in intact $\alpha L\beta 2$, substitution of Ile-306 with alanine increased adhesion to ICAM-1 (62). However, a soluble αL I domain truncated at residue 305 and hence lacking Ile-306 did not show increased affinity for ICAM-1 (M. Shimaoka and T. A. Springer, unpublished data). In isolated αL I domains, the C-terminal α -helix is mobile in NMR structures (44), shows variable conformations in crystal structures, and does not pack well against the body of the domain (42,43). Therefore, the effect on ligand binding of mutation of residue 306 in intact $\alpha L\beta 2$, but not in isolated I domains, suggests that the C-terminal α -helix is well packed against the body of the I domain in intact $\alpha L\beta 2$, and that interactions with other domains are important for the conformation of the C-terminal α -helix. Mutation in $\alpha L\beta 2$ of another hydrophobic residue in the same pocket underlying the C-terminal α -helix, I235A, activated ligand binding (62). Thus, in the context of intact $\alpha L\beta 2$, mutations in the hydrophobic pocket appear to favor the open conformation of the I domain.

In vivo experiments using antibodies and gene disruption have shown that binding of $\alpha L\beta 2$ to ICAMs is important in leukocyte trafficking in inflammation, lymphocyte homing, and T lymphocyte interactions with antigen-presenting cells in immune reactions (63,64). These findings suggested that antagonists of $\alpha L\beta 2$ could be useful for the therapy of autoimmune diseases. Indeed, a blocking mAb directed to the αL I domain was shown to be efficacious in phase 3 clinical studies of patients with psoriasis (65). High throughput screening of large chemical libraries has led to the identification by more than three different pharmaceutical companies of small molecules directed to the I domain that inhibit binding of $\alpha L\beta 2$ to ICAM-1 (45,66–71). The compounds are highly specific for $\alpha L\beta 2$ compared to $\alpha M\beta 2$. Remarkably, each of the independently discovered lead compounds, which belong to different chemical classes, binds to the hydrophobic pocket between the C-terminal α -helix and the β -sheet, as documented by three different companies using NMR or crystallography (45,69,71). This binding site is distant from the ligand-binding site at the MIDAS. Together with the finding that the drug–I domain complexes crystallize in the closed conformation, this suggests that the compounds allosterically

Table 1. The affinity for ICAM-1 of the locked open αL I domain is equal to that of intact $\alpha L\beta 2$

Immobilized ligand	Analyte	k_{on} ($M^{-1}s^{-1}$)	k_{off} (s^{-1})	K_D (μM)
sICAM-1	WT I domain	2950 ± 440	4.95 ± 0.85	1670 ± 100
sICAM-1	closed I domain	2110 ± 400	2.84 ± 0.27	1760 ± 70
sICAM-1	open I domain	139000 ± 8000	0.0257 ± 0.0015	0.185 ± 0.012
open I domain	sICAM-1	107000 ± 3000	0.0275 ± 0.0028	0.258 ± 0.024
$\alpha L\beta 2^a$	sICAM-1	224000 ± 69000	0.0298 ± 0.0069	0.133 ± 0.041

Binding kinetics were measured by surface plasmon resonance. Data are from (58), except for measurements on $\alpha L\beta 2$.

^a Data from (61).

inhibit binding to ICAM-1 by favoring the closed conformation. In agreement with this hypothesis, $\alpha\text{L}\beta 2$ containing a mutant I domain locked open with an engineered disulfide bridge as described above was completely resistant to inhibition by drug compound (59). In contrast, $\alpha\text{L}\beta 2$ heterodimers containing I domains of wild type or with single cysteine substitutions are susceptible to drug compound, as is $\alpha\text{L}\beta 2$ containing the locked open I domain after disulfide reduction with dithiothreitol. Thus, the drug compounds inhibit lymphocyte function-associated (LFA)-1 function by binding to the closed conformation of the I domain and by blocking the conformational transition to the open form that mediates adhesion to ICAMs. The ability of these compounds to inhibit cell adhesion *in vitro* and *in vivo* provides strong evidence that a change in affinity, and not a change in avidity through clustering on the cell surface, is responsible for physiologic regulation of adhesiveness.

Another class of compounds described by Genentech (San Francisco, CA, USA) (72) and Roche (Basel, Switzerland) (73) inhibit both $\alpha\text{L}\beta 2$ and $\alpha\text{M}\beta 2$ (73,74). Although claimed to mimic ICAM-1 by the Genentech group (75), the compounds do not bind either to the αL or αM I domains, but perturb binding of mAb to the $\beta 2$ I-like domain (74). Furthermore, the compound class inhibits binding by wild-type $\alpha\text{L}\beta 2$, but not by locked open $\alpha\text{L}\beta 2$, wild-type isolated I domain, or locked open isolated I domain (T. A. Springer, A. Salas and M. Shimaoka, unpublished data). Since the I domain is the binding site for ICAM-1 and the compounds do not bind to the I domain, they are not ICAM-1 mimics. The I-like domain of the $\beta 2$ subunit is a regulatory domain that does not participate directly in binding to ICAM-1 (60). The compounds have a crucial carboxyl group moiety that is likely to ligate to the MIDAS of the I-like domain, as shown for the carboxyl group of Arg-Gly-Asp (RGD)-like antagonists of integrins that lack I domains (16).

The mechanistic basis of I domain activation (bell-pull model)

The above studies demonstrate that I domain conformation dramatically regulates affinity for ligand, that the open conformation is sufficient to maximally activate cell adhesion independently of the transmembrane and cytoplasmic domains, that drug compounds that lock I domains in the closed conformation inhibit cell adhesion, and that antibodies detect changes on integrins in physiologically activated cells that are intrinsic to the integrin and not dependent on ligand binding. It is inescapable that regulation of I domain conformation regulates cell adhesion by integrins. Since we do not yet know

the structure of an I domain in the context of the $\alpha\beta$ heterodimer, the details of the interdomain contacts that convert the I domain into the active conformation are not clear. However, several clues point to a mechanism for I domain activation in the native receptor.

The C-terminal linker connecting the I domain to the β -propeller domain is much longer than the N-terminal linker. In the primary structure of the α subunit, the I domain is inserted between blades (β -sheets) 2 and 3 of the β -propeller domain, with its N-terminus immediately following the last β -strand (β -strand 4) of blade 2. A pair of cysteines conserved only among I domain-containing α subunits is predicted to form a disulfide that connects the loop between β -strands 2 and 3 in blade 2 to the segment that follows β -strand 4 in blade 2. There are only three residues from this disulfide-bridged cysteine to the first residue defined in I domain structures, indicating that the N-terminus of the I domain is closely tethered to the β -propeller domain. However, the C-terminal linker of the I domain is much longer, and thus may permit much greater conformational motion. This linker is ~ 20 amino acid residues long, and connects the end of the C-terminal α -helix of the I domain to β -strand 1 in blade 3 of the β -propeller. Many of the residues are serines, suggesting flexibility.

Since the closed conformation is favored energetically in isolated I domains and appears to be the default conformation adopted in the basal, inactive state of integrins on the cell surface, conversion to the open conformation would require an external input of energy. This energy would have to come from movements at interdomain contacts. The most likely type of motion is a downward movement of the C-terminal α -helix, which could be induced by exertion of a bell-rope-like pull on a segment within the C-terminal linker region (Fig. 8). The signals could be propagated via the C-terminal linker sequence to the C-terminal α -helix, and thence to the MIDAS.

Consistent with the bell-rope model, mutation of exposed residues near the bottom of the I domain and in the linker region can regulate ligand binding. In one study, 17 sequence segments distributed over all faces of the human αM I domain were swapped with corresponding mouse segments (54). Of these, only three substitutions, all located on the bottom face, increased binding to ligand and expression of the CBRM1/5 activation epitope. In another investigation (76), two segments at the bottom of the αM I domain were swapped with corresponding segments of the αL I domain; each swap activated ligand binding. Interestingly, similar substitutions at the bottom of the von Willebrand factor A1 domain, which is

highly homologous to integrin I domains, have been found to activate ligand binding and result in spontaneous binding of von Willebrand factor to platelets (77).

Mutational and antibody epitope studies also support a role for the C-terminal linker region in regulating ligand binding by the I domain and in conformational movements. The last α -helical residue defined in I domain structures is equivalent to Tyr-307 in α L; Ser-327 approximates the beginning of the β -propeller domain, leaving a linker of residues 308–326. Some mutations in this linker sequence, K314A and L317A, activate ligand binding by α L β 2, while other mutations at the linker, Y307A and E310A, inactivate α L β 2 (62). This finding suggests that contacts between the linker and other domains modulate the conformation of the I domain. In further support of conformational movement of the linker region, CBR LFA-1/1, a conformation-sensitive α L mAb (78), maps to residues 301–338, which include all of the linker and the last two turns of the C-terminal α -helix (59,79).

What pulls the bell-rope, i.e. the C-terminal linker? The integrin α subunit β -propeller and I domains are in close proximity to the β subunit I-like domain. In the crystal structure of integrin α V β 3 (11), the MIDAS of the β subunit I-like domain is positioned very close to the loop in the β -propeller in which the I domain is inserted. It is possible that the open and closed conformations of the I domain are regulated by interaction of the C-terminal linker with the β -propeller and/or the I-like domain at this site. Since this site is equivalent to the ligand-binding site in integrins that lack I domains, alterations in the interaction of the linker with the MIDAS of the I-like domain may occur that are analogous to those that regulate interactions with ligands in integrins that lack I domains. In summary, we predict that three structural units, the

I, β -propeller, and I-like domains, make a ternary interaction interface where structural rearrangements of the latter two domains affect the conformation of the I domain. More details of this structural rearrangement are presented in the last section of this review.

Conformational activation of the entire integrin heterodimer

The mystery of global conformational change in integrins. The platelet integrin α IIb β 3 is one of the most extensively studied non-I domain integrins, and it has been known for more than a decade that it undergoes large conformational change during affinity up-regulation or upon ligand binding (13,80,81). This change can be reported by binding of mAbs specific for the activated or ligand-bound conformation; frequently these mAbs map to the C-terminal cysteine-rich domains in the β subunit, quite distant from the ligand binding site (82–84). Global conformational change is not specific to β 3 integrins, but it is shared by other members of the integrin family including those that contain I domains (39,85,86). The fact that most of these “conformation specific” mAbs could also induce high-affinity ligand binding suggested that the activation of integrins on the cell surface is accomplished by conformational modulation of extracellular domains of integrin also in the physiologic setting, when this is induced by signals from inside the cells (inside-out signaling). A “hinge” hypothesis was introduced as a mechanism of this conformational activation, where a site of association between the cytoplasmic tails of α and β subunits acts like a fulcrum that allows separation of head domains of both subunits upon receiving the cellular signal (87,88). Many mutations in the cytoplasmic domains of α and β subunits alter ligand-binding activity, supporting the role of the cytoplasmic tails (89–94). A modified version of this hypothesis was presented, where the fulcrum is actually located in the integrin headpiece rather than in the transmembrane domains, and intersubunit dissociation at the transmembrane and/or cytoplasmic domain opens the stalks, allowing the conversion of the ligand-binding headpiece to the high-affinity conformation (14,95). However, this “stalk-opening” hypothesis is not without a caveat, because it does not explain the strange fact that the activation-dependent mAbs are almost exclusively against the β subunit.

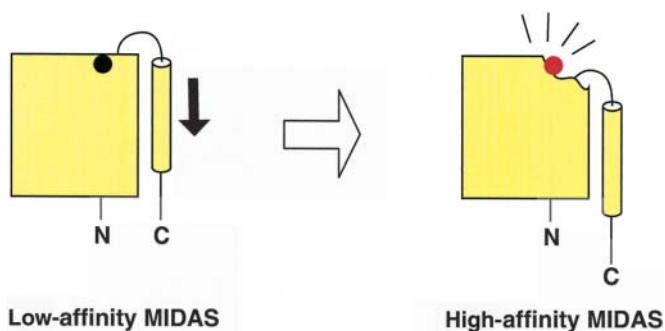


Fig. 8. Bell-rope model of conformational activation of the integrin I domain. The main body of the I domain is depicted as a rectangle, with the C-terminal α -helix (shown as a cylinder) connected via a loop. Conformational change around the MIDAS metal (sphere) activating ligand binding is induced by the downward pull of the C-terminal α -helix.

Crystal structure of α V β 3 integrin

The structure of the α V β 3 extracellular segment reveals a surprising bent conformation (Fig. 1B), where the ligand-bind-

ing headpiece is folded back onto the tailpiece of the molecule, so that on the cell surface the ligand-binding site would be facing the membrane surface near the transmembrane domains (11). It was suggested that the bent conformation was less likely to exist on the cell surface, implying that it was a crystal packing artifact. However, the size of the interface buried between the headpiece and the tailpiece as a consequence of the bend at the genu is 1400 \AA^2 , and it is thus in the range expected for physiologic interactions rather than crystal

packing artifacts. If the bent conformation is physiologically relevant, then another issue remains unanswered: is it in the active or resting state? Although it was suggested by Xiong et al. that the ligand-binding domains were in an active conformation (11), this state would appear to be in contradiction to the overall conformation of the integrin in which they are present, which would orient the ligand-binding site toward the membrane, a topology unfavorable for binding to ligands in the extracellular matrix or on the surface of other cells. A structure of $\alpha V\beta 3$ complexed with cyclic RGD peptide ligand was recently reported (16), and also assumes the bent conformation. In this study, however, crystals formed in the absence of ligand were soaked in a buffer containing a high concentration of ligand peptide, preventing a global conformational rearrangement. So the issue of the physiological relevance of the bent form remained unresolved.

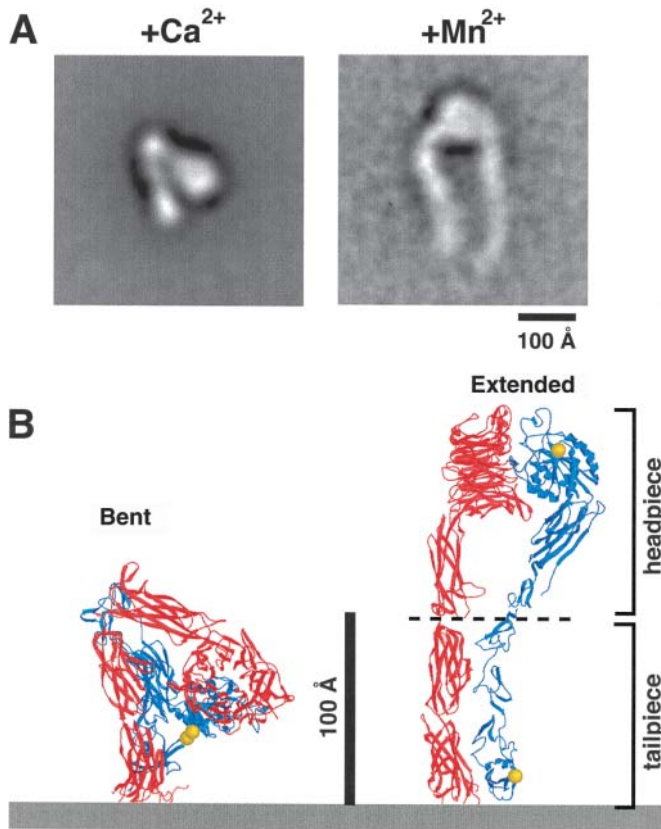


Fig. 9. Bent and extended conformations of the $\alpha V\beta 3$ integrin. **A**) Recombinant soluble $\alpha V\beta 3$ in the presence of Ca^{2+} (left) or Mn^{2+} (right) were observed under EM after negative stain (17). Projection averages obtained from 769 (Ca^{2+}) or 104 (Mn^{2+}) representative particles are shown. Bar: 100 Å. **B**) Ribbon diagrams of the alternative conformations of the extracellular segment of $\alpha V\beta 3$ integrin. αV is red and $\beta 3$ is blue. The bent conformation observed in the crystal structure (11) with I-EGF domains 1, 2, and a portion of 3 built in, similar to the model described in (19), is shown on the left, and a corresponding model of the extended conformation is shown on the right. The model of the unbent molecule was created by breaking the bent form at the junction between the thigh and calf-1 domains in α and I-EGF1 and 2 in β (dashed line) into the headpiece and tailpiece, and moving the headpiece relative to the tailpiece. The approximate position of the cell membrane is indicated by a gray line. The black bar indicates 100 Å. Gold spheres show the $\text{C}\alpha$ positions of residues that, when mutated to cysteine, form a disulfide bond that restrains $\alpha V\beta 3$ and $\alpha \text{IIb}\beta 3$ in an inactive state (17).

Two conformations seen in electron microscopy (EM) We recently observed recombinant soluble $\alpha V\beta 3$ protein under EM after negative staining (17). In the presence of Ca^{2+} , the $\alpha V\beta 3$ molecule shows a compact V-shaped appearance with a size and shape identical to that reported in the crystal structure (Fig. 9A). One leg of the V ends in a large globule corresponding to the integrin headpiece, while the other leg corresponds to the tailpiece. The tip of the V corresponds to the genu. The angle between the legs of the V in the crystal structure and that in the EM projections are the same, showing that the degree of bending is not a crystal structure artifact. The bent conformation thus represents the predominant native conformation of $\alpha V\beta 3$ in Ca^{2+} . In sharp contrast, the same preparation shows a very different, completely extended conformation in the presence of Mn^{2+} , a known strong activator of integrins (Fig. 9A). The dominant structure is a globular head with two long tails, which is very similar to the electron micrograph images previously reported for native or recombinant integrins after rotary shadowing (12–14,96,97). These results show that exposure of $\alpha V\beta 3$ to Mn^{2+} induces breakage of the large interface between the headpiece and tailpiece in the bent conformation, and the straightening of the bend at the genu.

Is the global change in integrin conformation relevant for regulation of affinity for ligand?

The above study demonstrated that $\alpha V\beta 3$ undergoes a global conformational change between the Ca^{2+} -bound and Mn^{2+} -bound states. Since it is known that Ca^{2+} and Mn^{2+} act as negative and positive regulators for integrin activity, respectively, it was important to test whether shape-shifting be-

tween these two conformations was responsible for affinity regulation. The hypothesis is very similar to that addressed above, that different conformations of the integrin I domain differ in affinity for ligand. This time the extent of conformational change is much larger; nonetheless, approaches similar to those used for I domains were used to address the physiological significance of global conformational change.

Ligand binding was measured with surface plasmon resonance using exactly the same $\alpha V\beta 3$ preparations as examined above by EM. The two different conformers differ dramatically in ligand-binding activity. Ligand binding by $\alpha V\beta 3$ in physiological concentrations of Ca^{2+} and Mg^{2+} (1 mM each) is almost negligible, but is of high affinity in buffer containing 1 mM Mn^{2+} (17). Therefore, conversion of $\alpha V\beta 3$ by Mn^{2+} to the extended conformation is accompanied by a dramatic increase in affinity for its physiologic ligand fibronogen.

The bent form of $\alpha V\beta 3$ in the crystal study was suggested to be in an active conformation by the authors (11). This assumption was based on the fact that the recombinant $\alpha V\beta 3$ used in crystallization showed strong ligand-binding activity in the presence of 1 mM Ca^{2+} in a solid-phase binding assay (98). However, the integrin was coated onto the plastic surface in the presence of 10 μM Mn^{2+} , which would convert $\alpha V\beta 3$ into the active, extended form. The hydrophobic interaction to the plastic surface would have maintained the active conformation of the immobilized integrin even after the removal of the Mn^{2+} ion. In agreement with our own findings, Smith et al. (99) have reported that Ca^{2+} cannot support ligand binding of solution phase $\alpha V\beta 3$ purified from placenta. We find that direct immobilization of integrins onto plastic surfaces activates them for binding to soluble ligands in buffer containing Ca^{2+} and Mg^{2+} (100). This finding is in sharp contrast to the lack of ligand binding by the same integrin preparations in solution phase in Ca^{2+} and Mg^{2+} measured using surface plasmon resonance, and it suggests that immobilization by absorption to a surface induces conformational change and, hence, activation of integrins. The fact that a peptide ligand can bind to the bent conformation of $\alpha V\beta 3$ in crystals (16) does not show that this conformation represents a physiological activated state, since high concentrations of peptide ligand can bind to inactive integrins (101).

Both $\alpha V\beta 3$ and $\alpha IIb\beta 3$ assume the bent conformation on the cell surface (17). Val-332 and Ser-674 of the $\beta 3$ subunit are predicted to be far apart in the $\beta 3$ subunit in the extended conformation, but in the bent conformation the C β atoms of these residues are only 5.6 Å apart (Fig. 9B). When these two residues are mutated to cysteines, they form a disulfide bond.

Because disulfide bond formation is 100% complete in the context of both $\alpha V\beta 3$ and $\alpha IIb\beta 3$, it is likely that the bent conformation is the major default conformation of $\beta 3$ integrins on the cell surface.

Finally and most importantly, $\alpha V\beta 3$ and $\alpha IIb\beta 3$ integrins, locked in the bent conformation by the engineered disulfide bond described above, were inactive in cell adhesion assays under basal conditions and resistant to activation by Mn^{2+} and activating mAbs, unless the disulfide bond reducing reagent dithiothreitol was added (17). These observations show that integrins on the surface of resting cells are essentially completely present in the bent conformation and that a conformational rearrangement involving movement apart of the headpiece and tailpiece is required for integrin activation.

A switchblade-like model for integrin activation

Conformational change from the bent to an extended structure nicely explains the heavy bias toward anti- β over anti- α mAbs among activation-reporting mAbs. In the bent $\alpha V\beta 3$ structure, the β subunit is innermost in the bend (Figs 9B and 10). About 70% of the solvent-accessible surface area that is buried in the headpiece–tailpiece interface is contributed by the β subunit. The β subunit PSI domain and integrin EGF domains 1, 2, and a portion of 3 are missing from the $\alpha V\beta 3$ structure, and these domains would further increase the contribution of the β subunit to the headpiece–tailpiece interface (19). Once the integrin undergoes conformational change to the extended structure, the newly exposed surface should thus be mainly composed of the β subunit.

Recently, we have determined the NMR solution structure of integrin-EGF module 3 of the $\beta 2$ subunit and obtained perturbation spectra for the tandem pair of modules 2 and 3 that allowed us to build a model of these two domains (19). $\beta 2$ I-EGF modules 2 and 3 were superimposed on the partial I-EGF3 module in $\alpha V\beta 3$. The $\alpha V\beta 3/\beta 2$ combined model allows the orientation of functionally important residues to be visualized, and it provides strong support for the idea that the bent conformation represents the inactive conformation. Residues in $\beta 2$ I-EGF module 3, which restrain integrins in the inactive state and had been predicted to be in an $\alpha\beta$ interface (30), are on the face pointing towards calf domain 1 of the α subunit stalk (black spheres, Fig. 10). The residues participating in the KIM127 activation epitope in $\beta 2$ I-EGF module 2 (purple spheres) and in the CBR LFA-1/2 and MEM48 activation epitopes in I-EGF module 3 (cyan spheres) are masked in the bent conformation (Fig. 10). However, in the extended, unbent conformation, there is no domain that could mask these epitopes. The transition from the bent to

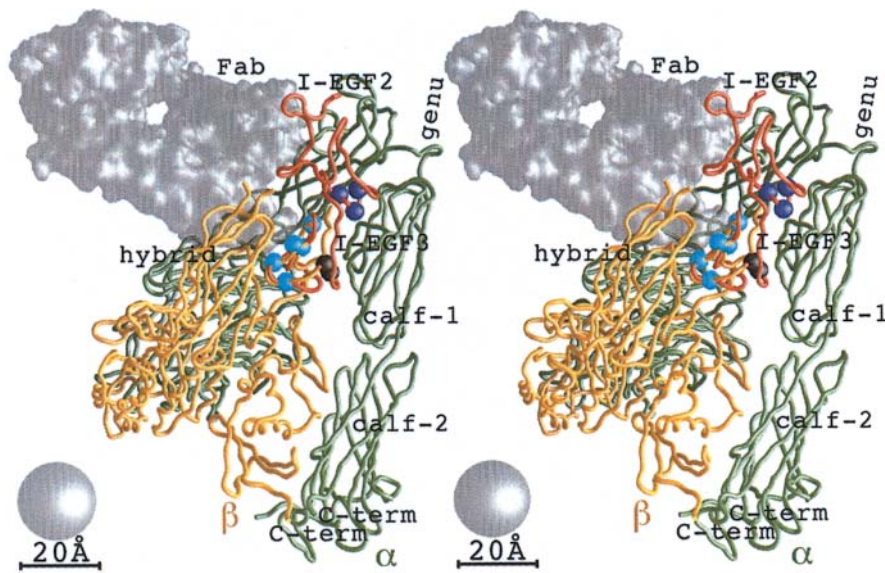


Fig. 10. Activation-related residues in the β subunit stalk are hidden in the bent form.

Stereo backbone ribbon traces of $\beta 2$ I-EGF2+3 (19) and $\alpha V\beta 3$ (11) are shown. Polypeptide backbones are red for $\beta 2$ I-EGF2+3, green for αV , and yellow for $\beta 3$. Alpha carbon atoms of residues in the KIM127 epitope (Gly 504, Leu 506 and Tyr 508) are purple, and in the CBR LFA-1/2 (Leu 534, Phe 536 and His 543) and MEM48 (also includes Arg 541 and Phe 546) epitopes, the alpha carbons are cyan (39). Alpha carbon atoms of residues that restrain activation of human $\alpha X\beta 2$ (Gln 525 and Val 526) and were suggested to be in an $\alpha\beta$ interface are black (30). The surface of a representative Fab antibody fragment (gray; pdb accession number 1A3R), with its antigen-binding site oriented toward and at closest approach to the KIM127 and CBR LFA1/2 epitopes, is shown to illustrate that the KIM127 and CBR LFA-1/2 epitopes are inaccessible to its antigen-binding site. A gray sphere 20 Å in diameter is included at the bottom left as a size reference. Figure from ref (19).

the extended conformation provides a mechanism for unmasking of these activation epitopes. In $\beta 3$, a mutation has been identified that results in a constitutively active $\alpha IIb\beta 3$ receptor (102). This mutation (T562N) introduces an unnatural N-glycosylation site at the center of the interaction between I-EGF modules 3 and 4 in the β tailpiece and the hybrid domain in the β headpiece, and it is predicted to force open the headpiece–tailpiece leading to constitutive activity.

On the basis of these observations, we conclude that integrin activation involves a switchblade-like motion in which the interface between the headpiece and tailpiece is broken, and the headpiece moves from a position close to the plasma membrane (Fig. 11, left) to one in which it is exposed for efficient interactions with ligands on other cells or in the extracellular matrix (Fig. 11, right) (17,19). Our findings show that breaking the interface between the headpiece and the tailpiece is a key step in the pathway of integrin activation. This is consistent with a large body of evidence suggesting that, on the cell surface, interactions between juxtamembrane segments of the integrin α and β subunits stabilize the inactive state. In the resting state on the cell surface, there may be breathing at the headpiece–tailpiece interface, with an equilibrium between fully and partially bent conformations, where the equilibrium is in favor of the fully bent form and binding of activating antibodies to the interface can favor opening. Once the intersubunit restraint at the transmembrane/cytoplasmic domain is released

by cellular mechanisms, the equilibrium would shift towards the extended conformer.

Previously, integrins have been imagined to be in an extended conformation in the resting state. This thought has posed the perplexing question of how conformational signals could be transmitted over the long distance of 150 Å from the membrane to the headpiece. The bent conformation provides a solution to this problem. Conformational movements need only be transmitted from the membrane to the headpiece–tailpiece interface, a much shorter distance. Subsequent to movement apart of the α and β subunit cytoplasmic/transmembrane domains, movement apart of the C-terminal segments of the α and β subunits in the tailpiece would destabilize the interface with the headpiece, and open the switch blade (Fig. 11).

A model for activation of the β subunit I-like domain
The remaining question to answer is why the bent form has low affinity for ligand. At first glance, it seems as if the folding of the ligand-binding headpiece against the lower portion of the stalks and the close apposition of the headpiece to the membrane simply renders the binding site sterically inaccessible to macromolecular ligands. This simple masking of the binding site is, however, unlikely to be the only mechanism responsible for the low affinity of the bent conformer for ligands. Masking by the membrane cannot explain our obser-

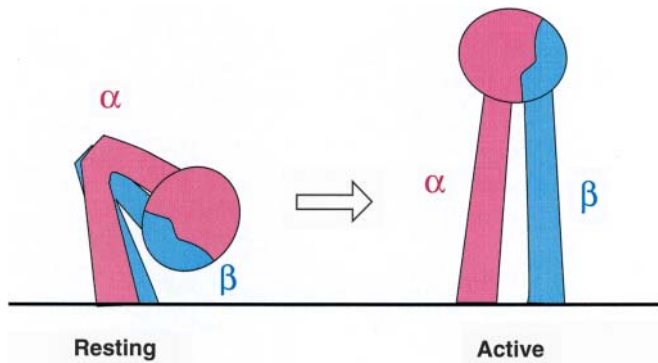


Fig. 11. Model for integrin activation by global conformational change. The model of the resting integrin resembles the form of $\alpha V\beta 3$ observed in the crystal structure (11); the active integrin is depicted in an extended conformation as seen in electron micrographs of $\alpha V\beta 3$ in the presence of Mn^{2+} .

vation that a soluble form of bent $\alpha V\beta 3$ has low affinity for ligand (17). Therefore, unbending may only be the first step in the integrin activation pathway and may facilitate further steps. Interestingly, the majority of the projection averages for $\alpha V\beta 3$ in Mn^{2+} show a larger angle between the stalks below the globular head than in the crystal structure (17). As the ligand-binding surface is located on the top of the globular head, opposite the face where the stalks are connected, it is intriguing to speculate that this opening of the upper stalks converts the ligand-binding site to the high-affinity state. The I-like domain is connected through both its N- and C-termini to the hybrid domain. Since the C-terminus of the β I-like domain is located closer to the α subunit, swinging the hybrid domain away from the α subunit would automatically pull down the C-terminal α -helix of the I-like domain (Fig. 12A). Conversely, downward movement of the C-terminal α -helix would swing the hybrid domain away from the α subunit, as observed in the EM images of activated $\alpha V\beta 3$. By analogy to I domain activation induced by downward movement of the C-terminal α -helix as discussed above, we predict that activation of the I-like domain for ligand binding is linked to a downward movement in its C-terminal α -helix and a corresponding change in orientation between the hybrid and I-like domains. We note that the hybrid domain is prominent in the headpiece–tailpiece interface, and that this interface restrains the orientation of the hybrid domain to the I-like domain. This provides a mechanism for linking opening of this interface to conformational movements in the I-like domain, and vice versa. It is significant that, among all integrin domains, it is only the I domain in the α subunit and the I-like domain in the β subunit that are inserted within

other domains, therefore possessing two covalent connections to the same domain.

A model for activation of the α subunit I domain in the context of an intact integrin heterodimer

Early on, it was thought that, in I domain-containing integrins, the I-like domain in the β subunit made a direct contribution to ligand binding, because mutations in the MIDAS of the I-like domain, and mAb directed to the I-like domain, inhibited ligand binding. However, as described above, the isolated αL I domain, when locked in the open conformation, is sufficient to give a binding affinity equivalent to that of activated $\alpha L\beta 2$ and also to give equivalent adhesiveness when present on the cell surface. Remarkably, ligand binding by $\alpha L\beta 2$ containing an I domain locked open with a disulfide is completely resistant to inhibition by mAbs to the $\beta 2$ I-like domain that fully inhibit ligand binding by activated wild-type $\alpha L\beta 2$, and bind equally well to locked open and wild-type $\alpha L\beta 2$ (60). These mAb were mapped to multiple epitopes located in three widely separated sites on the molecular surface of the I-like domain of $\beta 2$ (103). Furthermore, disulfide reduction with dithiothreitol restored the susceptibility of the disulfide-locked receptor to the inhibitory mAbs, showing that the mutant receptors override the blocking effect of mAbs because their conformation is fixed. This clearly demonstrates that the mAbs to the $\beta 2$ I-like domain inhibit by an allosteric mechanism rather than by directly competing with the ligand. Thus, in $\beta 2$ integrins, the I-like domain does not directly participate in ligand binding, and appears to affect ligand binding indirectly by regulating the conformation of the I domain (60).

Observations on the effect of Ca^{2+} and Mn^{2+} ions on ligand binding by I domain-containing integrins also favor a regulatory rather than a direct role for the β subunit I-like domain. High concentrations of Ca^{2+} are known to be inhibitory against many I domain-containing integrins. The Ser and Thr sidechains in the MIDAS strongly disfavor coordination to Ca^{2+} , which prefers more polar oxygen atoms. Furthermore, in contrast to results with intact $\alpha 2\beta 1$ and $\alpha L\beta 2$, binding of isolated $\alpha 2$ (104) and αL (M. Shimaoka and T. A. Springer, unpublished data) I domains to their ligands is not inhibited by mM concentrations of Ca^{2+} . Moreover, Mn^{2+} , a well-known strong activator of integrins, does not appear to activate by binding to the MIDAS of the I domain for three reasons: (i) Mn^{2+} -loaded αM and αL I domains crystallize in the closed conformation (40,43); (ii) the wild-type isolated I domain shows equivalent adhesiveness in Mg^{2+} and Mn^{2+} (105), and (iii) the locked open αL I domain shows identical

affinities and adhesiveness to ICAM-1 in Mg^{2+} and Mn^{2+} (M. Shimaoka and T. A. Springer, unpublished data).

The I-like domain is the best candidate for mediating the effects of Mn^{2+} and Ca^{2+} . A recently described Ca^{2+} -binding site in the I-like domain of the $\alpha V\beta 3$ structure is adjacent to the MIDAS of the I-like domain, and thus it has been termed the ADMIDAS (11). The ADMIDAS and the MIDAS of the I-like domain are likely to be the inhibitory Ca^{2+} - and stimulatory Mn^{2+} -binding sites. Based on the evidence described above that the I-like domain plays a regulatory rather than a direct role in ligand binding by I domain-containing integrins, we propose the following model for the function of the I-like domain in integrins that contain I domains

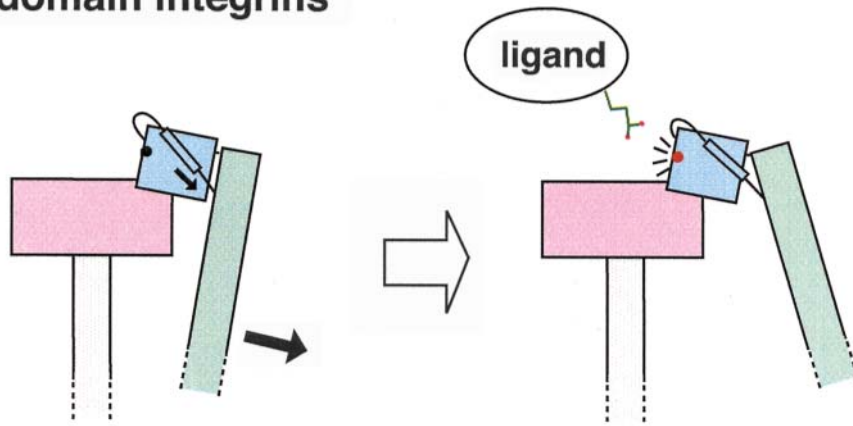
(Fig. 12B). We think that, in the active conformation of the I-like domain, it binds to a ligand-like segment in the α subunit, most likely in the I domain linker, and thereby exerts the downward pull on the bell-rope that remotely opens the conformation of the ligand-binding site of the I domain.

The relative importance of conformational change and clustering in inside-out and outside-in signaling

Inside-out signaling: affinity or avidity?

In this review, we have focused on regulation of the ligand-binding activity of an integrin by conformational shape-shifting within a single receptor molecule. However, many reports

A) Non-I domain integrins



B) I domain integrins

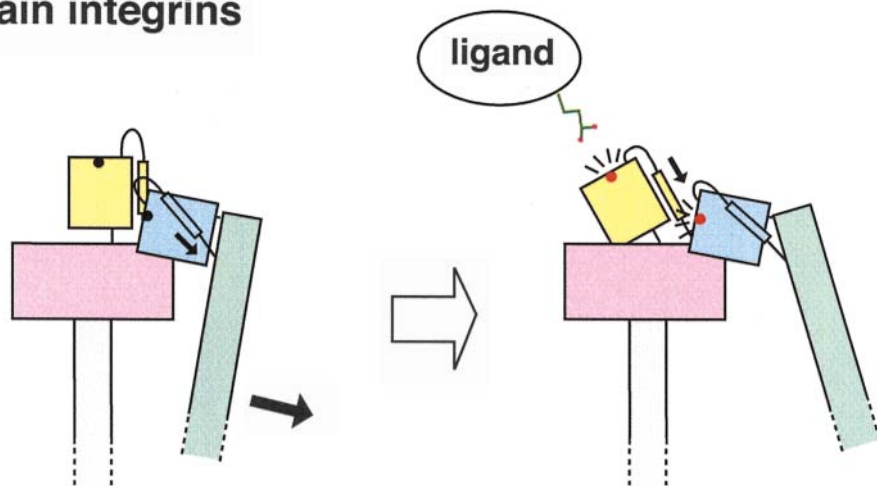


Fig. 12. Hypothetical model of conformational activation of integrins. A) In non-I domain integrins, swinging away the hybrid domain (light green) pulls the C-terminal α -helix of the I-like domain (light blue), converting the low-affinity MIDAS (black dot) to the high-affinity MIDAS (red dot) which is ready for direct interaction with

an acidic residue in the ligand protein. **B)** In I-domain containing integrins, the same movement activates the I-like domain MIDAS in the β subunit, which in turn ligates and pulls the C-terminal α -helix of the I domain, converting the I domain MIDAS to the high-affinity conformation that is ready for interaction with ligand.

suggest that up-regulation of integrin-mediated adhesion by activated cells is achieved by receptor clustering on the cell surface (i.e. avidity augmentation) rather than by, or together with, an increase in affinity of individual receptors (6–10). Clustering of receptors on the cell surface would no doubt increase overall cell adhesive efficiency, particularly when the ligands are di- or multivalent, and have a similar clustered distribution on the opposing cell or substrate. However, experimental evidence for the formation of integrin clusters on activated cells is rather qualitative, and in most cases is demonstrated experimentally by either a large dot-like or polarized staining pattern after cell fixation. Furthermore, it is difficult to know whether clustering triggers ligand binding, or is a result of ligand binding that is triggered by an increase in receptor affinity. Receptors on cells, including integrins, are well known to redistribute to sites on cells where they can bind ligand, as a consequence of their “capture” in ligand–receptor complexes. Moreover, real-time imaging has shown that the formation of visible clusters in adhering cells occurs long after the first contacts are made (106,107), while the ligand-binding activity of integrins on circulating cells such as leukocytes and platelets must be up-regulated in a matter of seconds *in vivo*.

Intermediate affinity states?

Avidity regulation has been adopted as an alternative to affinity regulation as the explanation for increased cellular adhesiveness, not because it has been directly demonstrated, but because in some instances there is a lack of evidence for affinity regulation. Affinity alteration has been dismissed as the mechanism of increased cell adhesion in these instances, based on the inability to detect increased binding of soluble ligands to cells that clearly exhibit increased adhesiveness (9). In some cases certain stimuli that cause increased cellular adhesiveness do result in a measurable increase in soluble ligand binding (affinity regulation is inferred) and other stimuli that also cause increased cell adhesiveness do not augment soluble ligand binding (avidity regulation is inferred) (7,8,108). The observation that the affinity of the α L I domain for ligand can range all the way from a K_D of 200 nM for the locked open I domain to 2 mM for the wild-type or locked closed I domain suggests that the lack of binding of soluble ligand should be interpreted with great caution (58). The K_D of 200 nM of the locked open I domain is just barely within the range that is detectable by conventional assays for ligand binding to cells. A K_D just 10-fold higher of 2 μ M would not be detectable by direct ligand binding to cells. However, cell adhesion does

not require high affinity (low K_D); for example, a K_D of 25 μ M is quite sufficient to mediate adhesion (109).

It is very reasonable to propose that, in integrin heterodimers on the cell surface, I domains could exist not just in two affinity states with K_D of 200 nM (open) and K_D of 2 mM (closed), but also in many intermediate states. This could result from equilibration between two states, with the affinity representing the time-averaged population of the 2 states, from the existence of true conformational intermediates along the shape-shifting pathway, or from differences in the kinetics of I domain opening. Activation of α L β 2 on the cell surface to an intermediate affinity with a K_D of 20 μ M for ICAM-1 would not be detectable by ligand binding to cells, but should be sufficient to activate cell adhesion, based on measurements with other cell adhesion molecules. Thus, conformational alterations in integrins resulting in an intermediate affinity for ligand could be the initial event in “inside-out” activation, which would allow cells to surmount the threshold from a nonadhesive to an adhesive phenotype. After cells make the initial contact to the ligand-bearing surface, clustering of integrins may further stabilize the adhesion machinery. Both stabilization of the active conformation of the integrin with bound ligand, as evidenced by ligand-induced binding site epitopes, and clustering of integrins may contribute to outside-in signaling.

Summary and extension of the model for integrin activation

To summarize, structures have been determined and models built for integrin I domains in two different conformations, open and closed. Mutational and functional studies demonstrate that the open conformation binds ligand with high affinity, and the closed conformation either does not bind ligand or binds with low affinity. In physiologic activation of integrins on the cell surface, studies with antibodies demonstrate that conformational change precedes ligand binding. However, it is not known whether these changes correspond precisely to transition from the closed to the open conformation of the I domain or transition to an intermediate conformation, since thus far the open conformation has been visualized only in the presence of a ligand or ligand-mimetic. The structural changes in I domains are similar to those in small G-proteins, particularly around the metal-binding site; however, metal-binding site rearrangement is linked to large motions in different backbone segments. C-terminal α -helix movement does not occur in G-proteins.

In I domains, the linkage to the C-terminal α -helix segment

provides a mechanism for propagating conformational change from one domain to another. Locking in alternate conformations of the loop preceding this C-terminal α -helix demonstrates that conformational movement here is linked to a dramatic 9000-fold increase in affinity of the ligand-binding site around the MIDAS. The C-terminal linker of the I domain is located in an interface between the β -propeller and I-like domains that constitutes the ligand-binding site in integrins that lack I domains. Interactions at this site of the linker in integrins that contain I domains may mimic interactions with ligands in integrins that lack I domains, and provide a mechanism for transmitting conformational motion.

EM images and crystal structures of $\alpha V\beta 3$, and NMR data on I-EGF modules 2 and 3 of $\beta 2$, show that integrin activation involves a dramatic conformational rearrangement from a bent to an extended conformation. In the inactive conformation, the headpiece faces the membrane. In activation, the headpiece extends upward in a switchblade-like motion. The headpiece–tailpiece interface is broken, and activation epitopes are exposed. These long-range rearrangements of the global interdomain architecture are coupled to conformational changes within the I and I-like domains, and probably also in adjacent loops in the β -propeller domain, that increase affinity for ligand. EM images suggest a change in orientation between the I-like and hybrid domains that is consistent with downward movement of the C-terminal α -helix of the I-like domain, analogous to the movement observed in the I domain. The double connections of the I domain and I-like domains to their neighboring domains in the α and β subunits, respectively, provide a mechanism for coupling conformational change within domains in integrins to global rearrangements in the orientation between domains. A complex between a small cyclic RGD peptide and the low-affinity conformation of $\alpha V\beta 3$ reveals coordination of the Asp carboxyl group with the MIDAS of the I-like domain. This is analogous to coordination to ligands observed with I domains in the high-affinity conformation, except for one crucial difference. In the I domain–ligand complexes, the ligand car-

boxyl is the only charged group in contact with the metal, providing a strong metal–ligand bond. However, in the I-like domain–ligand complex, a carboxyl group from the I-like domain also forms a direct coordination to the metal in the MIDAS, which would lower the strength of the bond to the RGD ligand. This is consistent with our observation that the bent $\alpha V\beta 3$ conformation has low affinity for ligand. We predict (i) that conversion to the high-affinity state occurs upon rearrangement of the coordination at the MIDAS of the I-like domain, such that the only carboxyl group directly coordinating to the metal is that contributed by the RGD ligand, and (ii) that this rearrangement at the MIDAS is tightly linked to a downward movement of the C-terminal α -helix of the I-like domain, providing a mechanism for linking the change in affinity for ligand to global integrin conformational change. Coupling of such a rearrangement to global conformational change in integrins is consistent with the ability of RGD-mimetics to induce ligand-induced binding site epitopes. In the context of physiologic activation of integrins, intracellular signaling cascades appear to cause repositioning of the juxtamembrane segments of the α and β subunits, which initiates the rearrangements in the extracellular domain.

Exactly how integrin heterodimers achieve signal transduction in both directions and the details of signal transmission between domains within these complex molecular machines await further biochemical, structural, and cell biological studies. The complexities of these molecules are appropriate to the sophisticated and diverse functions they mediate in connecting the intracellular and extracellular environments. Much more remains to be learned about how these molecules function in general, as well as about how different integrin heterodimers are specialized for diverse tasks. There is no doubt that the understanding of these events at the molecular level will reveal further exciting biological and structural principles, and will also greatly advance our ability to devise therapeutics to control the pathophysiology mediated by this important family of cell adhesion molecules.

References

1. Hynes RO. Integrins. Versatility, modulation, and signaling in cell adhesion. *Cell* 1992;**69**:11–25.
2. Humphries MJ. Integrin structure. *Biochem Soc Trans* 2000;**28**:311–339.
3. Bennett JS, Vilaire G. Exposure of platelet fibrinogen receptors by ADP and epinephrine. *J Clin Invest* 1979;**64**:1393–1401.
4. Dustin ML, Springer TA. T cell receptor cross-linking transiently stimulates adhesiveness through LFA-1. *Nature* 1989;**341**:619–624.
5. Diamond MS, Springer TA. The dynamic regulation of integrin adhesiveness. *Curr Biol* 1994;**4**:506–517.
6. Loftus JC, Smith JW, Ginsberg MH. Integrin mediated cell adhesion: the extracellular face. *J Biol Chem* 1994;**269**:25235–25238.

7. Faull RJ, Kovach NL, Harlan HM, Ginsberg MH. Stimulation of integrin-mediated adhesion of T lymphocytes and monocytes: two mechanisms with divergent biological consequences. *J Exp Med* 1994;**179**:1307–1316.
8. Stewart M, Hogg N. Regulation of leukocyte integrin function: affinity vs. avidity. *J Cell Biochem* 1996;**61**:554–561.
9. Bazzoni G, Hemler ME. Are changes in integrin affinity and conformation overemphasized? *Trends Biochem Sci* 1998;**23**:30–34.
10. van Kooyk Y, van Vliet SJ, Figdor CG. The actin cytoskeleton regulates LFA-1 ligand binding through avidity rather than affinity changes. *J Biol Chem* 1999;**274**:26869–26877.
11. Xiong J-P, et al. Crystal structure of the extracellular segment of integrin $\alpha V\beta 3$. *Science* 2001;**294**:339–345.
12. Weisel JW, Nagaswami C, Vilaire G, Bennett JS. Examination of the platelet membrane glycoprotein IIb–IIIa complex and its interaction with fibrinogen and other ligands by electron microscopy. *J Biol Chem* 1992;**267**:16637–16643.
13. Du X, et al. Long range propagation of conformational changes in integrin $\alpha_{\text{IIb}}\beta_3$. *J Biol Chem* 1993;**268**:23087–23092.
14. Takagi J, Erickson HP, Springer TA. C-terminal opening mimics ‘inside-out’ activation of integrin $\alpha 5\beta 1$. *Nat Struct Biol* 2001;**8**:412–416.
15. Takagi J, Debottis DP, Erickson HP, Springer TA. The role of specificity-determining loop of the integrin β -subunit I-like domain in folding, association with the α subunit, and ligand binding. *Biochemistry* 2002;**41**:4339–4347.
16. Xiong JP, et al. Crystal structure of the extracellular segment of integrin $\alpha V\beta 3$ in complex with an Arg-Gly-Asp ligand. *Science* 2002;**296**:151–155.
17. Takagi J, Petre BM, Walz T, Springer TA. A global conformational rearrangement in $\beta 3$ integrins regulates affinity for ligands. *Cell* 2002, in press.
18. de Pereda JM, Wiche G, Liddington RC. Crystal structure of a tandem pair of fibronectin type III domains from the cytoplasmic tail of integrin $\alpha 6\beta 4$. *EMBO J* 1999;**18**:4087–4095.
19. Beglova N, Blacklow SC, Takagi J, Springer TA. Cysteine-rich module structure reveals a fulcrum for integrin rearrangement upon activation. *Nat Struct Biol* 2002;**9**:282–287.
20. Springer TA. Folding of the N-terminal, ligand-binding region of integrin α -subunits into a β -propeller domain. *Proc Natl Acad Sci USA* 1997;**94**:65–72.
21. Oxvig C, Springer TA. Experimental support for a β -propeller domain in integrin α -subunits and a calcium binding site on its lower surface. *Proc Natl Acad Sci USA* 1998;**95**:4870–4875.
22. Springer TA, Jing H, Takagi J. A novel Ca^{2+} -binding β -hairpin loop better resembles integrin sequence motifs than the EF-hand. *Cell* 2000;**102**:275–277.
23. Kamata T, Tieu KK, Springer TA, Takada Y. Amino acid residues in the αIIb subunit that are critical for ligand binding to integrin $\alpha \text{IIb}\beta 3$ are clustered in the β -propeller model. *J Biol Chem* 2001;**276**:44275–44283.
24. Michishita M, Videm V, Arnaout MA. A novel divalent cation-binding site in the A domain of the $\beta 2$ integrin CR3 (CD11b/CD18) is essential for ligand binding. *Cell* 1993;**72**:857–867.
25. Diamond MS, Garcia-Aguilar J, Bickford JK, Corbi AL, Springer TA. The I domain is a major recognition site on the leukocyte integrin Mac-1 (CD11b/CD18) for four distinct adhesion ligands. *J Cell Biol* 1993;**120**:1031–1043.
26. Lee J-O, Rieu P, Arnaout MA, Liddington R. Crystal structure of the A domain from the α subunit of integrin CR3 (CD11b/CD18). *Cell* 1995;**80**:631–638.
27. Lu C, Oxvig C, Springer TA. The structure of the β -propeller domain and C-terminal region of the integrin αM subunit. *J Biol Chem* 1998;**273**:15138–15147.
28. Bork P, Doerks T, Springer TA, Snel B. Domains in plexins: links to integrins and transcription factors. *Trends Biochem Sci* 1999;**24**:261–263.
29. Calvete JJ, Henschen A, González-Rodríguez J. Assignment of disulphide bonds in human platelet GPIIIa. A disulphide pattern for the β -subunits of the integrin family. *Biochem J* 1991;**274**:63–71.
30. Zang Q, Springer TA. Amino acid residues in the PSI domain and cysteine-rich repeats of the integrin $\beta 2$ subunit that restrain activation of the integrin $\alpha X\beta 2$. *J Biol Chem* 2001;**276**:6922–6929.
31. Ponting CP, Schultz J, Copley RR, Andrade MA, Bork P. Evolution of domain families. *Adv Protein Chem* 2000;**54**:185–244.
32. Huang C, Lu C, Springer TA. Folding of the conserved domain but not of flanking regions in the integrin $\beta 2$ subunit requires association with the α subunit. *Proc Natl Acad Sci USA* 1997;**94**:3156–3161.
33. Huang C, Springer TA. Folding of the β -propeller domain of the integrin $\alpha 4$ subunit is independent of the I domain and dependent on the $\beta 2$ subunit. *Proc Natl Acad Sci USA* 1997;**94**:3162–3167.
34. Puzon-McLaughlin W, Kamata T, Takada Y. Multiple discontinuous ligand-mimetic antibody binding sites define a ligand binding pocket in integrin $\alpha \text{IIb}\beta 3$. *J Biol Chem* 2000;**275**:7795–7802.
35. Zang Q, Lu C, Huang C, Takagi J, Springer TA. The top of the I-like domain of the integrin LFA-1 β subunit contacts the α subunit β -propeller domain near β -sheet 3. *J Biol Chem* 2000;**275**:22202–22212.
36. Yuan Q, Jiang W-M, Leung E, Hollander D, Watson JD, Krissansen GW. Molecular cloning of the mouse integrin $\beta 7$ subunit. *J Biol Chem* 1992;**267**:7352–7358.
37. Takagi J, Beglova N, Yalamanchili P, Blacklow SC, Springer TA. Definition of EGF-like, closely interacting modules that bear activation epitopes in integrin β subunits. *Proc Natl Acad Sci USA* 2001;**98**:11175–11180.
38. Tan S-M, et al. Defining the repeating elements in the cysteine-rich region (CRR) of the CD18 integrin $\beta 2$ subunit. *FEBS Lett* 2001;**505**:27–30.
39. Lu C, Ferzly M, Takagi J, Springer TA. Epitope mapping of antibodies to the C-terminal region of the integrin $\beta 2$ subunit reveals regions that become exposed upon receptor activation. *J Immunol* 2001;**166**:5629–5637.
40. Lee J-O, Bankston LA, Arnaout MA, Liddington RC. Two conformations of the integrin A-domain (I-domain): a pathway for activation? *Structure* 1995;**3**:1333–1340.
41. Baldwin ET, et al. Cation binding to the integrin CD11b I domain and activation model assessment. *Structure* 1998;**6**:923–935.
42. Qu A, Leahy DJ. Crystal structure of the I-domain from the CD11a/CD18 (LFA-1, $\alpha 4\beta 2$) integrin. *Proc Natl Acad Sci USA* 1995;**92**:10277–10281.
43. Qu A, Leahy DJ. The role of the divalent cation in the structure of the I domain from the CD11a/CD18 integrin. *Structure* 1996;**4**:931–942.
44. Legge GB, et al. NMR solution structure of the inserted domain of human leukocyte function associated antigen-1. *J Mol Biol* 2000;**295**:1251–1264.
45. Kallen J, et al. Structural basis for LFA-1 inhibition upon lovastatin binding to the CD11a I-domain. *J Mol Biol* 1999;**292**:1–9.
46. Emsley J, King SL, Bergelson JM, Liddington RC. Crystal structure of the I domain from integrin $\alpha 2\beta 1$. *J Biol Chem* 1997;**272**:28512–28517.
47. Emsley J, Knight CG, Farnsdale RW, Barnes MJ, Liddington RC. Structural basis of collagen recognition by integrin $\alpha 2\beta 1$. *Cell* 2000;**101**:47–56.

48. Nolte M, Pepinsky RB, Venyaminov SY, Kotliansky V, Gotwals PJ, Karpusas M. Crystal structure of the $\alpha 1\beta 1$ integrin I-domain: insights into integrin I-domain function. *FEBS Lett* 1999;**452**:379–385.
49. Rich RL, et al. Trench-shaped binding sites promote multiple classes of interactions between collagen and the adherence receptors, $\alpha 1\beta 1$ integrin and *Staphylococcus aureus* Cna MSCRAMM. *J Biol Chem* 1999;**274**:24906–24913.
50. Liddington R, Bankston L. The integrin I domain: crystals, metals and related artefacts. *Structure* 1998;**6**:937–938.
51. Staunton DE, Dustin ML, Erickson HP, Springer TA. The arrangement of the immunoglobulin-like domains of ICAM-1 and the binding sites for LFA-1 and rhinovirus. *Cell* 1990;**61**:243–254.
52. Lollo BA, Chan KWH, Hanson EM, Moy VT, Brian AA. Direct evidence for two affinity states for lymphocyte function-associated antigen 1 on activated T cells. *J Biol Chem* 1993;**268**:21693–21700.
53. Diamond MS, Springer TA. A subpopulation of Mac-1 (CD11b/CD18) molecules mediates neutrophil adhesion to ICAM-1 and fibrinogen. *J Cell Biol* 1993;**120**:545–556.
54. Oxvig C, Lu C, Springer TA. Conformational changes in tertiary structure near the ligand binding site of an integrin I domain. *Proc Natl Acad Sci USA* 1999;**96**:2215–2220.
55. Shimaoka M, Shifman JM, Jing H, Takagi J, Mayo SL, Springer TA. Computational design of an integrin I domain stabilized in the open, high affinity conformation. *Nat Struct Biol* 2000;**7**:674–678.
56. Dahiyat BI, Mayo SL. De novo protein design: fully automated sequence selection. *Science* 1997;**278**:82–87.
57. Xiong J-P, Li R, Essafi M, Stehle T, Arnaout MA. An isoleucine-based allosteric switch controls affinity and shape shifting in integrin CD11b A-domain. *J Biol Chem* 2000;**275**:38762–38767.
58. Shimaoka M, Lu C, Palframan R, von Andrian UH, Takagi J, Springer TA. Reversibly locking a protein fold in an active conformation with a disulfide bond: integrin α L I domains with high affinity and antagonist activity in vivo. *Proc Natl Acad Sci USA* 2001;**98**:6009–6014.
59. Lu C, Shimaoka M, Ferzly M, Oxvig C, Takagi J, Springer TA. An isolated, surface-expressed I domain of the integrin $\alpha L\beta 2$ is sufficient for strong adhesive function when locked in the open conformation with a disulfide. *Proc Natl Acad Sci USA* 2001;**98**:2387–2392.
60. Lu C, Shimaoka M, Zang Q, Takagi J, Springer TA. Locking in alternate conformations of the integrin $\alpha L\beta 2$, I domain with disulfide bonds reveals functional relationships among integrin domains. *Proc Natl Acad Sci USA* 2001;**98**:2393–2398.
61. Labadia ME, Jeanfavre DD, Caviness GO, Morelock MM. Molecular regulation of the interaction between leukocyte function-associated antigen-1 and soluble ICAM-1 by divalent metal cations. *J Immunol* 1998;**161**:836–842.
62. Huth JR, et al. NMR and mutagenesis evidence for an I domain allosteric site that regulates lymphocyte function-associated antigen 1 ligand binding. *Proc Natl Acad Sci USA* 2000;**97**:5231–5236.
63. Springer TA. Traffic signals for lymphocyte recirculation and leukocyte emigration: the multi-step paradigm. *Cell* 1994;**76**:301–314.
64. Bouvard D, et al. Functional consequences of integrin gene mutations in mice. *Circ Res* 2001;**89**:211–223.
65. Gottlieb A, et al. Effects of administration of a single dose of a humanized monoclonal antibody to CD11a on the immunobiology and clinical activity of psoriasis. *J Am Acad Dermatol* 2000;**42**:428–435.
66. Kelly TA, et al. Cutting edge: a small molecule antagonist of LFA-1-mediated cell adhesion. *J Immunol* 1999;**163**:5173–5177.
67. Weitz-Schmidt G, et al. Statins selectively inhibit leukocyte function antigen-1 by binding to a novel regulatory integrin site. *Nat Med* 2001;**7**:687–692.
68. Liu G, et al. Discovery of novel p-arylthio cinnamides as antagonists of leukocyte function-associated antigen-1/intracellular adhesion molecule-1 interaction. 1. Identification of an additional binding pocket based on an anilino diaryl sulfide lead. *J Med Chem* 2000;**43**:4025–4040.
69. Last-Barney K, et al. Binding site elucidation of hydantoin-based antagonists of LFA-1 using multidisciplinary technologies: evidence for the allosteric inhibition of a protein-protein interaction. *J Am Chem Soc* 2001;**123**:5643–5650.
70. Woska JR Jr, Shih D, Taqueti VR, Hogg N, Kelly TA, Kishimoto TK. A small-molecule antagonist of LFA-1 blocks a conformational change important for LFA-1 function. *J Leukoc Biol* 2001;**70**:329–334.
71. Liu G, et al. Novel p-arylthio cinnamides as antagonists of leukocyte function-associated antigen-1/intracellular adhesion molecule-1 interaction. 2. Mechanism of inhibition and structure-based improvement of pharmaceutical properties. *J Med Chem* 2001;**44**:1202–1210.
72. Burdick DJ. Antagonists for treatment of CD11/CD18 adhesion receptor mediated disorders. PCT International Application WO9949856. San Francisco: Genentech; 1999.
73. Fotouhi N, Gillespie P, Guthrie R, Pietranico-Cole S, Yun W. Diaminopropionic acid derivatives. PCT International Application WO0021920. Basel: Hoffmann-La Roche; 1999.
74. Welzenbach K, Hommel U, Weitz-Schmidt G. Small molecule inhibitors induce conformational changes in the I domain and the I-like domain of lymphocyte function-associated antigen-1: molecular insights into integrin inhibition. *J Biol Chem* 2002;**277**:10590–10598.
75. Gadek TR, et al. Generation of an LFA-1 antagonist by the transfer of the ICAM-1 immunoregulatory epitope to a small molecule. *Science* 2002;**295**:1086–1089.
76. Zhang L, Plow EF. A discrete site modulates activation of I domains. *J Biol Chem* 1996;**271**:29953–29957.
77. Emsley J, Cruz M, Handin R, Liddington R. Crystal structure of the von Willebrand factor A1 domain and implications for the binding of platelet glycoprotein Ib. *J Biol Chem* 1998;**273**:10396–10401.
78. Ma Q, Shimaoka M, Lu C, Jing H, Carman CV, Springer TA. Activation induced conformational changes in the I domain region of LFA-1. *J Biol Chem* 2002;**277**:10638–10641.
79. Huang C, Springer TA. A binding interface on the I domain of lymphocyte function associated antigen-1 (LFA-1) required for specific interaction with intercellular adhesion molecule 1 (ICAM-1). *J Biol Chem* 1995;**270**:19008–19016.
80. Parise LV, Helgerson SL, Steiner B, Nannizzi L, Phillips DR. Synthetic peptides derived from fibrinogen and fibronectin change the conformation of purified platelet glycoprotein IIb-IIIa. *J Biol Chem* 1987;**262**:12597–12602.
81. Sims PJ, Ginsberg MH, Plow EF, Shattil SJ. Effect of platelet activation on the conformation of the plasma membrane glycoprotein IIb-IIIa complex. *J Biol Chem* 1991;**266**:7345–7352.
82. Honda S, et al. Topography of ligand-induced binding sites, including a novel cation-sensitive epitope (AP5) at the amino terminus, of the human integrin $\beta 3$ subunit. *J Biol Chem* 1995;**270**:11947–11954.
83. Frelinger AL, Lam SCT, Plow EF, Smith MA, Loftus JC, Ginsberg MH. Occupancy of an adhesive glycoprotein receptor modulates expression of an antigenic site involved in cell adhesion. *J Biol Chem* 1988;**263**:12397–12402.

84. Frelinger AL III, Du X, Plow EF, Ginsberg MH. Monoclonal antibodies to ligand-occupied conformers of integrin $\alpha_{IIb}\beta_3$ (glycoprotein IIb-IIIa) alter receptor affinity, specificity, and function. *J Biol Chem* 1991;**266**:17106–17111.
85. Bazzoni G, Shih D-T, Buck CA, Hemler MA. Monoclonal antibody 9EG7 defines a novel β_1 integrin epitope induced by soluble ligand and manganese, but inhibited by calcium. *J Biol Chem* 1995;**270**:25570–25577.
86. Yednock TA, et al. $\alpha_2\beta_1$ integrin-dependent cell adhesion is regulated by a low affinity receptor pool that is conformationally responsive to ligand. *J Biol Chem* 1995;**270**:28740–28750.
87. O'Toole TE, et al. Integrin cytoplasmic domains mediate inside-out signal transduction. *J Cell Biol* 1994;**124**:1047–1059.
88. Hughes PE, et al. Breaking the integrin hinge. *J Biol Chem* 1996;**271**:6571–6574.
89. Hibbs ML, Xu H, Stacker SA, Springer TA. Regulation of adhesion to ICAM-1 by the cytoplasmic domain of LFA-1 integrin beta subunit. *Science* 1991;**251**:1611–1613.
90. Lu C, Springer TA. The α subunit cytoplasmic domain regulates the assembly and adhesiveness of integrin lymphocyte function-associated antigen-1 (LFA-1). *J Immunol* 1997;**159**:268–278.
91. O'Toole TE, Mandelman D, Forsyth J, Shattil SJ, Plow EF, Ginsberg MH. Modulation of the affinity of integrin $\alpha_{IIb}\beta_3$ (GPIIb-IIIa) by the cytoplasmic domain of α_{IIb} . *Science* 1991;**254**:845–847.
92. Hughes PE, O'Toole TE, Ylanne J, Shattil SJ, Ginsberg MH. The conserved membrane-proximal region of an integrin cytoplasmic domain specifies ligand binding affinity. *J Biol Chem* 1995;**270**:12411–12417.
93. Kassner PD, Hemler ME. Interchangeable α chain cytoplasmic domains play a positive role in control of cell adhesion mediated by VLA-4, a β_1 integrin. *J Exp Med* 1993;**178**:649–660.
94. Kawaguchi S, Hemler ME. Role of the α subunit cytoplasmic domain in regulation of adhesive activity mediated by the integrin VLA-2. *J Biol Chem* 1993;**268**:16279–16285.
95. Lu C, Takagi J, Springer TA. Association of the membrane-proximal regions of the α and β subunit cytoplasmic domains constrains an integrin in the inactive state. *J Biol Chem* 2001;**276**:14642–14648.
96. Nermut MV, Green NM, Eason P, Yamada SS, Yamada KM. Electron microscopy and structural model of human fibronectin receptor. *EMBO J* 1988;**7**:4093–4099.
97. Wippler J, Kouns WC, Schaefer EJ, Kuhn H, Hadvary P, Steiner B. The integrin $\alpha_{IIb}\beta_3$, platelet glycoprotein IIb-IIIa, can form a functionally active heterodimer complex without the cysteine-rich repeats of the β_3 subunit. *J Biol Chem* 1994;**269**:8754–8761.
98. Mehta RJ, et al. Transmembrane-truncated $\alpha V\beta_3$ integrin retains high affinity for ligand binding: evidence for an 'inside-out' suppressor? *Biochem J* 1998;**330**:861–869.
99. Smith JW, Piotrowicz RS, Mathis D. A mechanism for divalent cation regulation of β_3 -integrins. *J Biol Chem* 1994;**269**:960–967.
100. Kohli RM, Takagi J, Walsh CT. The thioesterase domain from a nonribosomal peptide synthetase as a cyclization catalyst for integrin binding peptides. *Proc Natl Acad Sci USA* 2002;**99**:1247–1252.
101. Du X, Plow EF, Frelinger AL III, O'Toole TE, Loftus JC, Ginsberg MH. Ligands 'activate' integrin $\alpha_{IIb}\beta_3$ (platelet GPIIb-IIIa). *Cell* 1991;**65**:409–416.
102. Kashiwagi H, et al. A mutation in the extracellular cysteine-rich repeat region of the β_3 subunit activates integrins $\alpha_{IIb}\beta_3$ and $\alpha V\beta_3$. *Blood* 1999;**93**:2559–2568.
103. Huang C, Zang Q, Takagi J, Springer TA. Structural and functional studies with antibodies to the integrin β_2 subunit. a model for the I-like domain. *J Biol Chem* 2000;**275**:21514–21524.
104. Onley DJ, Knight CG, Tuckwell DS, Barnes MJ, Farndale RW. Micromolar Ca^{2+} concentrations are essential for Mg^{2+} -dependent binding of collagen by the integrin $\alpha_2\beta_1$ in human platelets. *J Biol Chem* 2000;**275**:24560–24564.
105. Knorr R, Dustin ML. The lymphocyte function-associated antigen 1, I domain is a transient binding module for intercellular adhesion molecule (ICAM)-1 and ICAM-1 in hydrodynamic flow. *J Exp Med* 1997;**186**:719–730.
106. Plancon S, Morel-Kopp MC, Schaffner-Reckinger E, Chen P, Kieffer N. Green fluorescent protein (GFP) tagged to the cytoplasmic tail of α_{IIb} or β_3 allows the expression of a fully functional integrin $\alpha_{IIb}\beta_3$. Effect of β_3 GFP on $\alpha_{IIb}\beta_3$ ligand binding. *Biochem J* 2001;**357**:529–536.
107. Laukaitis CM, Webb DJ, Donais K, Horwitz AF. Differential dynamics of α_5 integrin, paxillin, and α -actinin during formation and disassembly of adhesions in migrating cells. *J Cell Biol* 2001;**153**:1427–1440.
108. Constantin G, et al. Chemokines trigger immediate β_2 integrin affinity and mobility changes: differential regulation and roles in lymphocyte arrest under flow. *Immunity* 2000;**13**:759–769.
109. Dustin ML, et al. Low affinity interaction of human or rat T cell adhesion molecule CD2 with its ligand aligns adhering membranes to achieve high physiological affinity. *J Biol Chem* 1997;**272**:30889–30898.
110. Carson M. Ribbons. *Meth Enzymol* 1997;**277**:493–505.
111. Edwards CP, Fisher KL, Presta LG, Bodary SC. Mapping the intercellular adhesion molecule-1 and -2 binding site on the inserted domain of leukocyte function-associated antigen-1. *J Biol Chem* 1998;**273**:28937–28944.